α-Actinin-4/FSGS1 is required for Arp2/3-dependent actin assembly at the adherens junction

Vivian W. Tang and William M. Brieher

Department of Cell and Developmental Biology, University of Illinois, Urbana, IL 61801

We have developed an in vitro assay to study actin assembly at cadherin-enriched cell junctions. Using this assay, we demonstrate that cadherin-enriched junctions can polymerize new actin filaments but cannot capture preexisting filaments, suggesting a mechanism involving de novo synthesis. In agreement with this hypothesis, inhibition of Arp2/3-dependent nucleation abolished actin assembly at cell–cell junctions. Reconstitution biochemistry using the in vitro actin assembly assay identified α-actinin-4/focal segmental glomerulosclerosis 1 (FSGS1) as an essential factor. α-Actinin-4 specifically localized to sites of actin incorporation on purified membranes and at apical junctions in Madin–Darby canine kidney cells. Knockdown of α-actinin-4 decreased total junctional actin and inhibited actin assembly at the apical junction. Furthermore, a point mutation of α-actinin-4 (K255E) associated with FSGS failed to support actin assembly and acted as a dominant negative to disrupt actin dynamics at junctional complexes. These findings demonstrate that α-actinin-4 plays an important role in coupling actin nucleation to assembly at cadherin-based cell–cell adhesive contacts.

Introduction

Cadherins and actin collaborate during development to help polarize epithelial cells, fashion tissues, and shape whole embryos (Lecuit and Lenne, 2007). Cadherin–actin interactions continue to be important in the adult organism by providing strong cell–cell adhesion and mechanical support to maintain structural integrity as well as generation of cell shape during remodeling events such as wound healing and tissue regeneration (Gumbiner, 1996; Gumbiner, 2005). Actin filaments assemble beneath cadherin-mediated cell–cell contacts and concentrate in specialized cadherin-dependent junctions known as adherens junctions (McNeill et al., 1993; Bershadsky, 2004; Mège et al., 2006). Cadherins can even help govern the global organization of actin throughout an entire cell (Tao et al., 2007; Nandadasa et al., 2009). The actin cytoskeleton, in turn, helps determine the strength of cadherin-mediated adhesion (Angres et al., 1996; Imamura et al., 1999; Chu et al., 2004), and mechanical forces generated by the actin cytoskeleton can be transmitted to adjacent cells to reorganize a cell sheet or send a mechanical signal (Carramusa et al., 2007; Yonemura et al., 2010). Therefore, understanding cadherin-dependent biology requires a mechanistic understanding of how cadherin junctions help organize the actin cytoskeleton.

Many junctional proteins have been shown to be essential for the maintenance of an actin population at cadherin-mediated cell–cell contacts (Simske et al., 2003; Tinkle et al., 2008; Kwiatkowski et al., 2010; Xiao et al., 2010), but how actin is recruited and assembled at the junction is largely unknown. Genetic and cell biological approaches have implicated a long list of actin-binding proteins associated with cadherin junctions, which include α-catenin, vinculin, α-actinin, ZO-1, Eplin, and afadin (Wilkins and Lin, 1982; Hemmings et al., 1992; Rimm et al., 1995; Itoh et al., 1997; Mandai et al., 1997; Abe and Takeichi, 2008; Sawyer et al., 2009). This biochemical complexity reflects the diversity of actin-dependent processes occurring at these sites. For example, during gastrulation, cells within an interconnected sheet must establish new cadherin-mediated adhesions while dissolving others (Solnica-Krezel, 2006; Hammerschmidt and Wedlich, 2008; Montell, 2008). Initiation of a new cell–cell contact triggers local actin assembly (McNeill et al., 1993; Bershadsky, 2004; Mège et al., 2006). The contact point then matures, possibly connecting to a contractile

Correspondence to William M. Brieher: wbrieher@illinois.edu

Abbreviations used in this paper: EBSS, Earle's balanced salt solution; FSGS, focal segmental glomerulosclerosis; shRNA, short hairpin RNA; WT, wild type.

The Rockefeller University Press $30.00
J. Cell Biol. Vol. 196 No. 1 115–130
www.jcb.org/cgi/doi/10.1083/jcb.201103116

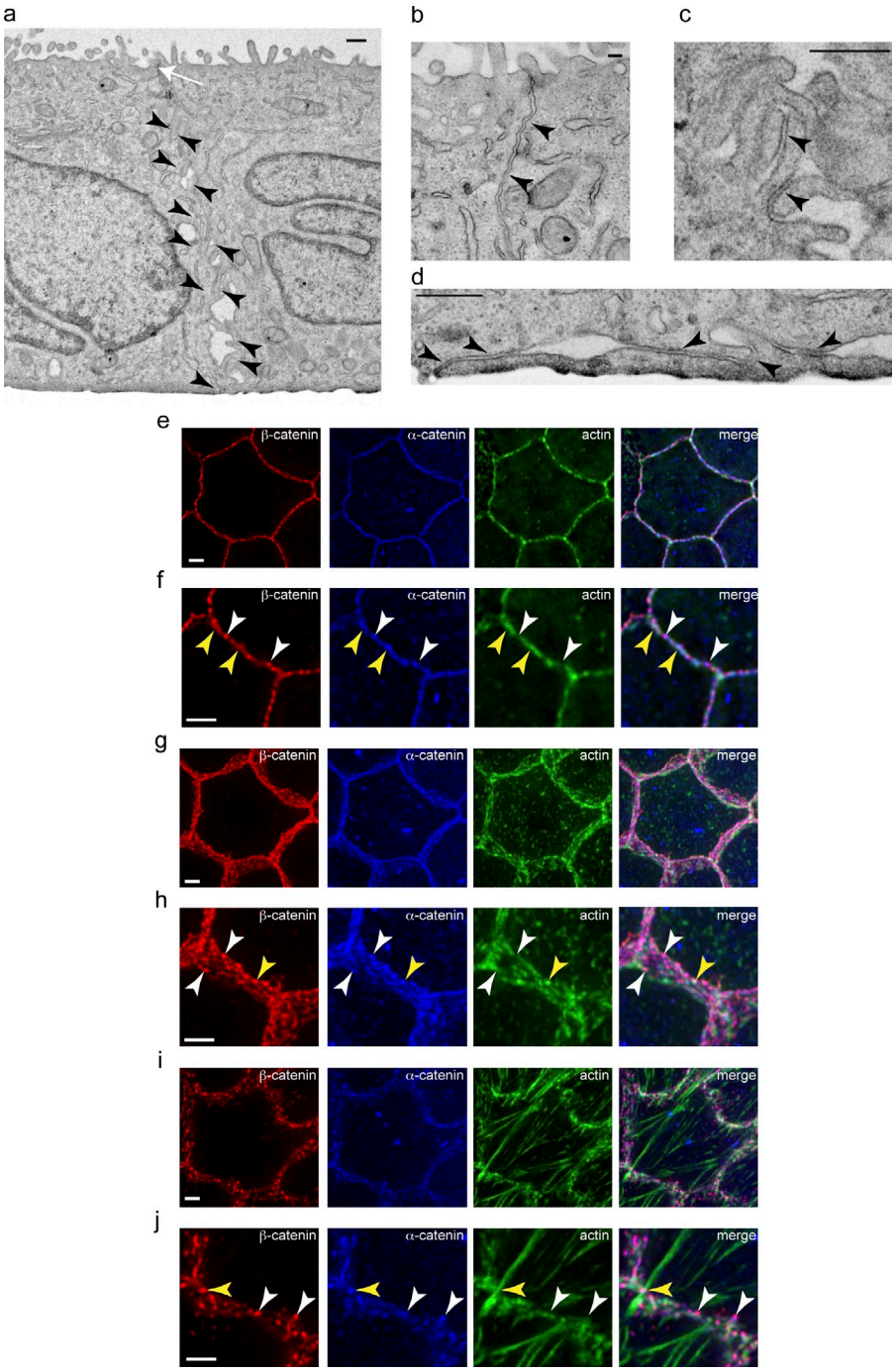

Figure 1. **Actin colocalizes with a subset of junctional complexes in polarized MDCK cells.** (a–d) Electron micrographs showing adherens junction (white arrow) and numerous interactions between adjacent cells along the lateral membrane (arrowheads; a). Cell–cell interactions are at apical (b), lateral (c), and basal membranes (d) of cells. Bars, 500 nm. (e and f) Single deconvolved optical z slices at the apical region of cells. (g and h) Projection of 35 deconvolved optical z slices spanning the apical 7 µm of cells. (i and j) Projection of the next 10 deconvolved optical z slices spanning 2 µm of the basal region of cells. (e–j) Yellow arrowheads point to areas where α-catenin (blue), β-catenin (red), and actin (phalloidin; green) are colocalized. White arrowheads point to areas where actin is missing from the α- and β-catenin puncta. Bars, 2 µm.

actomyosin network to help drive movement (Solnica-Krezel, 2006; Hammerschmidt and Wedlich, 2008; Montell, 2008). Finally, some contacts are dissolved and internalized, requiring a third actin organization at junctions to facilitate endocytosis (Ulrich and Heisenberg, 2009). Understanding the precise function of each of the various actin-binding proteins associated with cadherin cell–cell junctions will ultimately require biochemical analysis, but this process will not be as straightforward as might have been hoped. For example, α-catenin binds actin filaments in pure solution but fails to do so when incorporated into junctional complexes (Yamada et al., 2005; Kwiatkowski et al., 2010). Therefore, complex in vitro systems that reconstitute actin assembly reactions on cadherin-enriched membranes will be required to bridge genetic and cell biological work to future biochemical analysis in pure solution under defined conditions.

Most of the work examining cadherin–actin interactions has focused on developing embryos or cell culture models designed to mimic the initial phases of cell–cell contact and early steps in junctional maturation (Angres et al., 1996; Adams et al., 1998). Less is known regarding cadherin–actin interactions in mature junctions within highly differentiated tissues. However, understanding these interactions is important for human health, in which subtle mutations silent during embryogenesis might eventually compromise junction function over time, resulting in

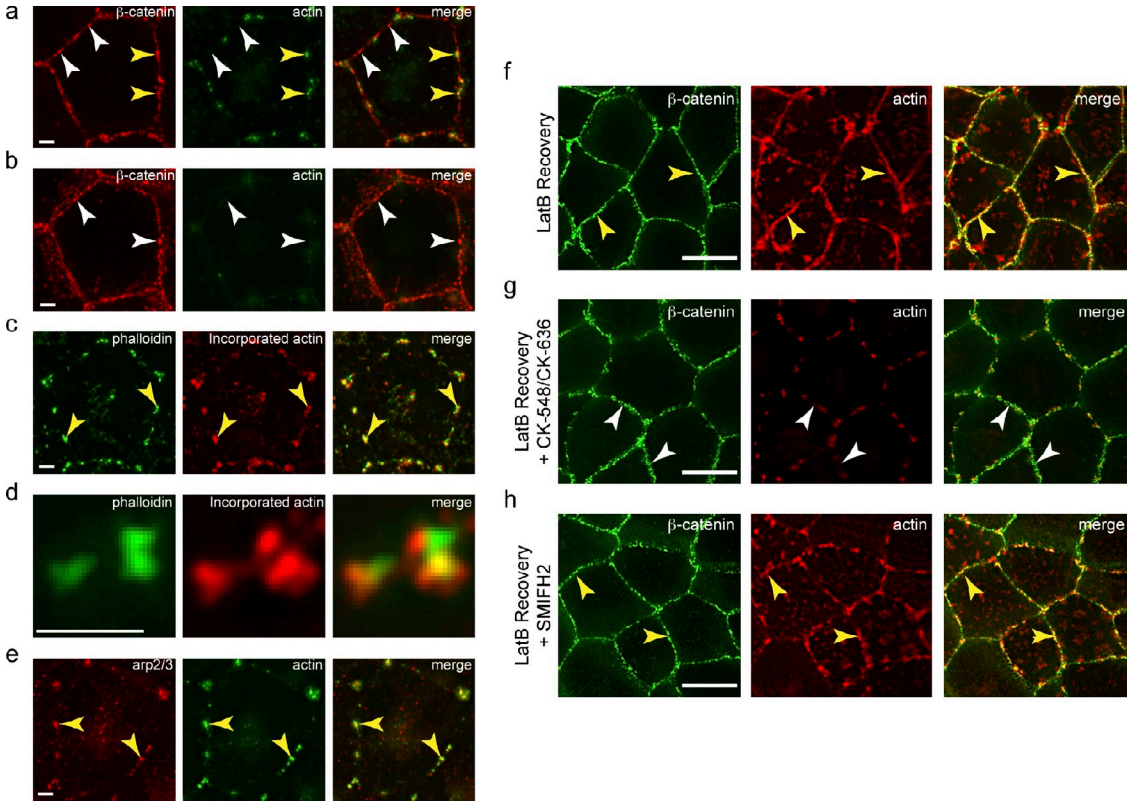

Figure 2. **Apical junction contains a latrunculin-resistant stable pool of actin that serves as sites of Arp2/3-dependent actin incorporation.** (a) Projection of the first 10 deconvolved optical z slices spanning 2 µm from the apical region of latrunculin-treated cells. (b) Projection of the next 30 deconvolved optical z slices spanning the next 6 µm of the basal regions of latrunculin-treated cells. (c and d) Single deconvolved optical z slices showing incorporation of fluorescently labeled actin (red) at latrunculin-stable actin puncta (phalloidin; green) in permeabilized cells (yellow arrowheads). (e) Arp3 (red) is colocalized (yellow arrowheads) with latrunculin-stable actin puncta (phalloidin; green). Projection of five deconvolved optical z slices spanning 1 µm from the apical region of cells. (a–e) Bars, 2 µm. (f) Projection of the first five deconvolved optical z slices spanning 1 µm from the apical region of cells after 30 min of latrunculin B (LatB) washout. (g) Projection of the first five deconvolved optical z slices spanning 1 µm from the apical region of cells 30 min after latrunculin washout in the presence of Arp2/3 inhibitors CK-548 and CK-636. (h) Projection of the first five deconvolved optical z slices spanning 1 µm from the apical region of cells 30 min after latrunculin washout in the presence of formin inhibitor SMIFH2. (a–c and f–h) Yellow arrowheads point to areas where β-catenin and actin (phalloidin) are colocalized. White arrowheads point to areas where actin is missing from β-catenin puncta. (f–h) Bars, 10 µm.

diseases in children or adults. Here, we examine mature cadherin-enriched cell–cell contacts in highly polarized MDCK cells to distinguish which, if any, cadherin junctions present in these cells are capable of assembling actin polymer. We then begin to dissect the biochemical requirements for assembling actin at cadherin-enriched foci by reconstituting the reaction using liver membranes.

Results

Sites of actin assembly in kidney epithelial cells

Polarized MDCK epithelial cells have distinct cell–cell adhesions distributed along the length of the lateral membrane (Fig. 1, a–d). The extent to which these adhesive sites colocalize with actin has not been examined. Therefore, we compared the distribution of α- and β-catenin relative to F-actin along the lateral membrane using deconvolution microscopy. We found that α-catenin, β-catenin, and actin are localized to overlapping yet distinct membrane puncta (Fig. 1, e–j). Apical and lateral catenins contain F-actin that appeared as puncta (Fig. 1, e–h), whereas basal F-actin appeared as bundles that are oriented perpendicular to the membrane (Fig. 1, i and j). Most of the laterally located catenins had either weak or no actin colocalization (Fig. 1, g and h). Using a whole-cell permeabilization assay (Turnacioglu et al., 1998; Vasioukhin et al., 2000; Zhang et al., 2005), we found that actin would incorporate into foci prominently at the apical and basal regions of the lateral membrane, suggesting junctional membranes serve as sites of actin assembly (Fig. S1).

A distinct pool of actin is thought to associate with spot adherens junctions in epithelial cells (Drenckhahn and Franz, 1986; Yonemura et al., 1995), and several studies had shown that a population of junction-associated actin is resistant to monomer sequestration by latrunculin (Yamada et al., 2004; Abe and Takeichi, 2008; Cavey et al., 2008). We found that polarized MDCK cells also have a latrunculin-resistant pool of actin at the apical junctions (Fig. 2 a). In contrast, actin on the lateral and basal regions was no longer detectable after latrunculin treatment (Fig. 2 b). Exogenous addition of fluorescently labeled actin would incorporate specifically at these latrunculin-stable foci (Fig. 2, c and d), suggesting that the apical junctions might serve as sites for actin nucleation. Immunofluorescence of the Arp3 subunit of the actin nucleator Arp2/3 complex showed

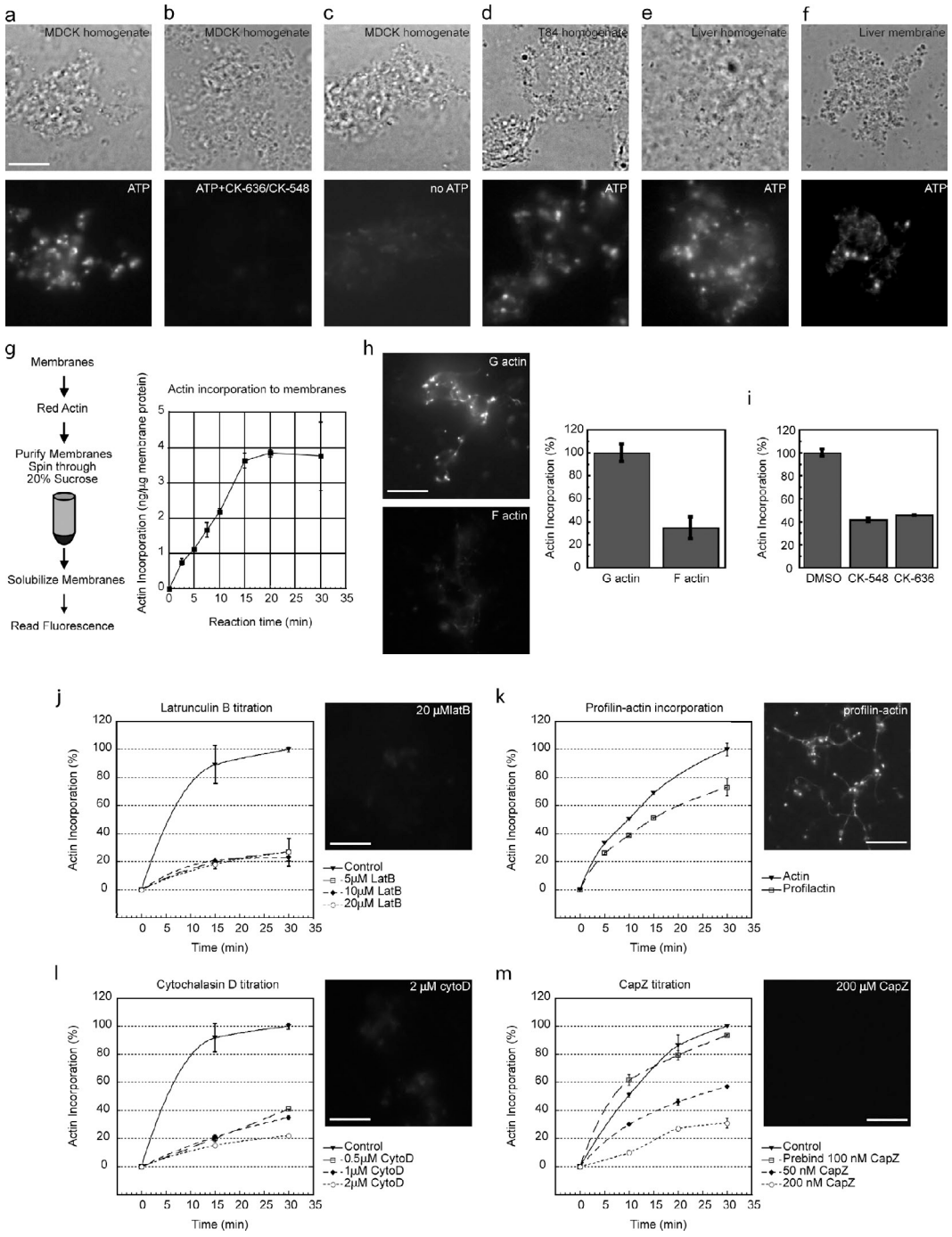

Figure 3. **Actin assembly on epithelial membranes requires Arp2/3 nucleation coupled to barbed-end growth.** (a–f) Fluorescently labeled actin is incorporated into membrane puncta in MDCK cell homogenate (a) but not in the presence of Arp2/3 inhibitors CK-636 and CK-548 (b) or in the absence of ATP (c). Fluorescently labeled actin is incorporated into membrane puncta in T84 intestinal epithelial cell homogenate (d), rat liver homogenate (e), and purified rat liver membranes (f). (g) Quantitation of actin incorporation. (h) Actin assembly on membranes can be supported by G-actin but not F-actin. (i) Actin incorporation to liver membranes is blocked by Arp2/3 inhibitor CK-548 or CK-636. (j) Latrunculin B inhibits actin assembly. (k) The profilin–actin complex supports actin assembly. (l) Cytochalasin D (Cyto D) inhibits actin assembly. (m) CapZ only inhibits actin assembly when present continuously. (g–m) Actin assembly reactions were performed in duplicates (g) and triplicates (h–m). Error bars represent SDs. Bars, 10 µm.

localization at these apical puncta (Fig. 2 e), implicating a role of Arp2/3 nucleation in actin assembly at the apical junction. Indeed, actin assembly (Fig. 2 f) was greatly retarded after latrunculin washout in the presence of Arp2/3 inhibitors CK-548 and CK-636 (Fig. 2 g; Nolen et al., 2009). Another actin nucleator, formin-1, has previously been shown to play a role in actin polymerization at nascent adherens junctions formed by keratinocytes (Kobielak et al., 2004). However, the addition of a broad-spectrum formin inhibitor, SMIFH2 (Rizvi et al., 2009), during latrunculin washout did not prevent actin recovery (Fig. 2 h).

We found that Arp2/3 and formin inhibition showed differential effects on the overall actin cytoskeleton of polarized

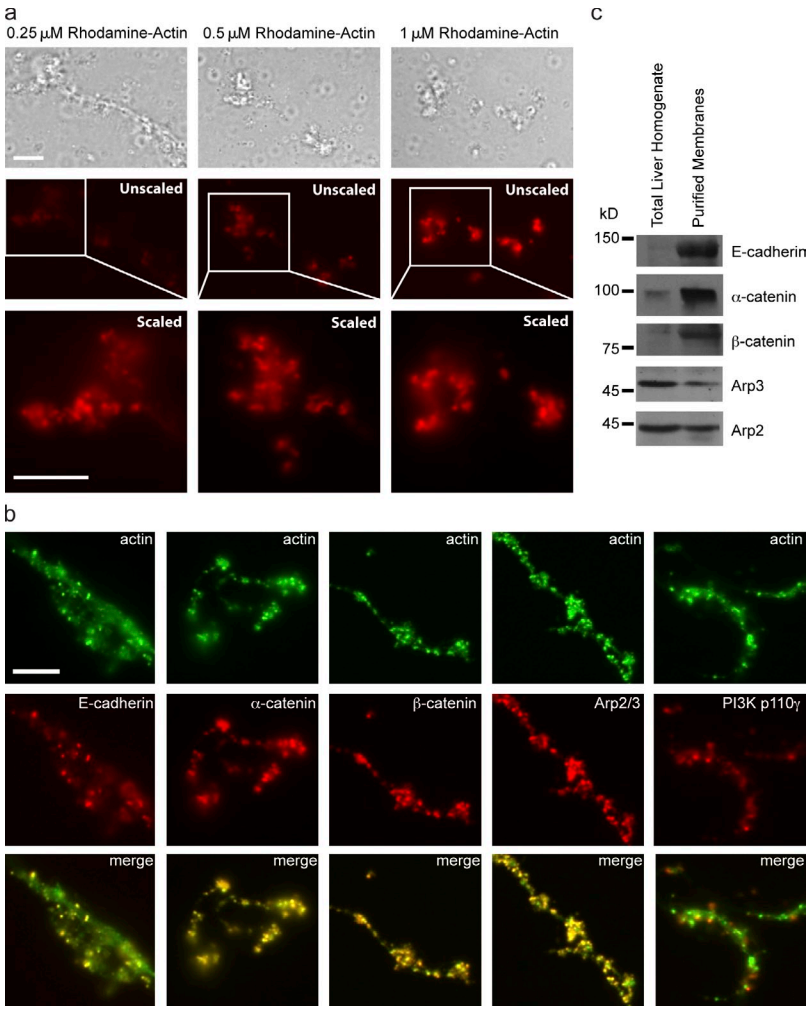

Figure 4. **E-cadherin–catenin–Arp2/3 puncta marked sites of actin assembly on purified membranes.** (a) Purified membranes were incubated with increasing concentrations of rhodamine-labeled G-actin. Although the total amounts of actin incorporated increased with actin concentration (unscaled), the sizes and numbers of membrane actin puncta were the same (scaled). Bar, 10 μm. (b) Immunofluorescence staining showing colocalization of actin puncta with E-cadherin, α-catenin, β-catenin, and Arp2/3 but not PI3K p110-γ. Bar, 5 μm. (c) Western blot of total liver homogenate and purified membrane fraction (see Materials and methods).

MDCK cells (Fig. S2). Arp2/3 inhibition by CK-548 greatly decreased the apical pool of actin without affecting the basal actin bundles (Fig. S2, c and d). On the other hand, formin inhibition by SMIFH2 had little effect on the apical actin population but eliminated most of the basal actin bundles (Fig. S2, e and f). In addition, formin-1 does not show strong colocalization with β-catenin and actin in polarized MDCK cells (Fig. S3). Therefore, formin-1 is unlikely to have primary roles in actin nucleation at the cadherin-based apical junction in polarized cells. On the other hand, the potent inhibition of actin recovery by Arp2/3 inhibitors and localization of Arp3 at latrunculin-stable foci strongly implicate an essential role of Arp2/3-dependent nucleation in actin assembly at the apical junction. However, it is difficult to distinguish whether actin nucleation occurs directly at junctional puncta or originates in the cytoplasm that was subsequently captured by the membrane complexes.

Actin assembly on epithelial cell membranes

The best way to distinguish between capturing versus polymerization at the membrane is to reconstitute the reaction in vitro. We started by adding fluorescently labeled monomeric actin and ATP to whole–MDCK cell homogenate. This resulted in labeling of membranes with actin puncta (Fig. 3 a). The labeling was inhibited by Arp2/3 inhibitors CK-548 and CK-636 (Fig. 3 b) and required ATP (Fig. 3 c). Homogenates of T84 intestinal epithelial cells and whole livers would also label membrane foci (Fig. 3, d and e), suggesting that actin incorporation is an universal property of epithelial membranes.

Although total cell homogenates can support actin assembly, we do not know whether the activity comes from the cytosol or the membrane itself. Therefore, we purified the membranes away from the cytosol and assayed for their actin incorporation activity. Combining differential centrifugation and equilibrium density gradients, eight membrane fractions were purified, and two fractions were capable of incorporating actin into puncta (Fig. S4). The majority of actin-incorporating activities reside in a major fraction consisting of large membranes, which will be used for further biochemical characterization (Fig. 3 f).

Quantitation of actin incorporation showed that the assembly reaction starts almost immediately upon monomer addition and continues linearly until it plateaus around 20 min (Fig. 3 g). In contrast, addition of filamentous actin to membranes did not support puncta formation (Fig. 3 h). Therefore, it is unlikely that filaments are formed de novo in solution and subsequently captured at specific membrane sites. Rather, actin incorporation into puncta requires direct polymerization at the membrane. Moreover, actin incorporation to membranes can be inhibited by CK-548 and CK-636 to the extent similar to the

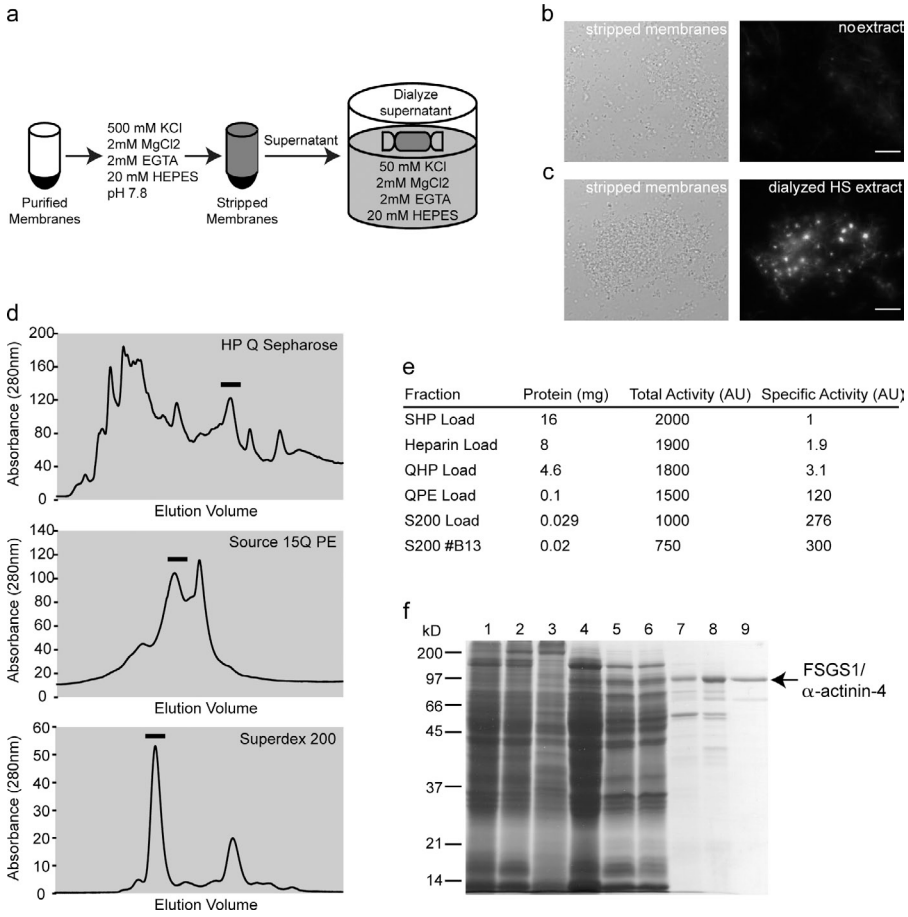

Figure 5. **Purification of high-salt–extractable actin assembly activity via biochemical reconstitution.** (a) Purified membranes were incubated in high salt to obtain a stripped membrane fraction and a high-salt fraction. (b) Stripped membranes cannot assemble actin. (c) Dialyzed high-salt (HS) extract rescued actin assembly on stripped membranes. (b and c) Bars, 10 µm. (d) The actin assembly activity from high-salt extract binds to Q HP and source Q columns and subsequently purified on Superdex 200. Bars on traces show fractions with activity. (e) Purification table for actin assembly activity. AU, arbitrary unit. (f) Coomassie blue–stained gel for the purification of actin assembly activity. Lane 1, homogenate; lane 2, purified membrane; lane 3, high-salt stripped membrane; lane 4, high-salt extract; lane 5, S and Blue flowthrough; lane 6, heparin flowthrough; lane 7, Q HP fractions with peak activity; lane 8, source Q fractions with peak activity; lane 9, Superdex 200 fraction B13 with peak activity. Q PE, quaternary ammonium polystyrene/divinylbenzene; SHP, sulfopropyl high performance.

published potency of these inhibitors (Nolen et al., 2009). Thus, both liver and MDCK membranes have similar properties for actin assembly, indicating that liver membranes would be useful for further biochemical investigation (Fig. 3 i).

Others had reported that cellular membranes have the capacity to bind actin monomers (Tranter et al., 1991; Cao et al., 1993). To rule out the possibility that actin was simply recruited to the membrane as monomers, we performed the assembly reaction in the presence of latrunculin, an actin monomer–sequestering drug that blocks polymerization (Morton et al., 2000). We found that actin incorporation on membranes was inhibited down to ∼20% by latrunculin (Fig. 3 j). The residual 20% incorporation represents diffuse fluorescence across the entire membrane but not bona fide assembly events.

Although unlikely, it is possible that monomers are adding to the pointed ends instead of the normally growing barbed ends. Therefore, we repeated the assay using preformed profilin–actin complexes that can only add to the barbed end (Pring et al., 1992; Kang et al., 1999). Profilin–actin was able to support membrane–actin puncta formation at a rate slightly slower than that of actin alone (Fig. 3 k). This is in agreement with published work that profilin–actin polymerizes at ∼85% of the rate of free actin (Pasic et al., 2008).

If membrane puncta formation is a result of monomer addition at the barbed end, barbed-end cappers such as cytochalasin D and CapZ should block actin assembly (Flanagan and Lin, 1980; Yamashita et al., 2003). Indeed, both cytochalasin D (Fig. 3 l) and CapZ (Fig. 3 m) inhibited actin incorporation in a dose-dependent manner. However, monomer growth from the barbed end can either result from nucleation or addition to preexisting filaments. To distinguish between these two possibilities, we blocked preexisting barbed ends with CapZ before testing for actin assembly. We found that actin incorporation was almost the same with or without CapZ pretreatment, suggesting that actin assembly is supported by de novo nucleation rather than growth from preexisting free barbed ends (Fig. 3 m).

Titration of actin concentrations revealed that the intensities of actin incorporated are proportional to the amounts of actin added (Fig. 4 a). However, the number and sizes of the actin foci are the same in all three actin concentrations, suggesting that the formation of foci is predetermined by factors on the membrane.

Cadherin–catenin–Arp2/3 complexes are sites of actin incorporation

Our earlier in vivo MDCK experiments indicated that discrete membrane adhesion complexes serve as sites for Arp2/3-dependent actin assembly. We found that junctional proteins and Arp2/3 colocalized with sites of actin incorporation on liver membranes, indicating that junctional foci are preserved in our biochemical purification procedure (Fig. 4 b). Western blot analysis confirmed that the purified liver membrane fraction contains Arp2/3 and was enriched in cadherin and α- and β-catenins (Fig. 4 c).

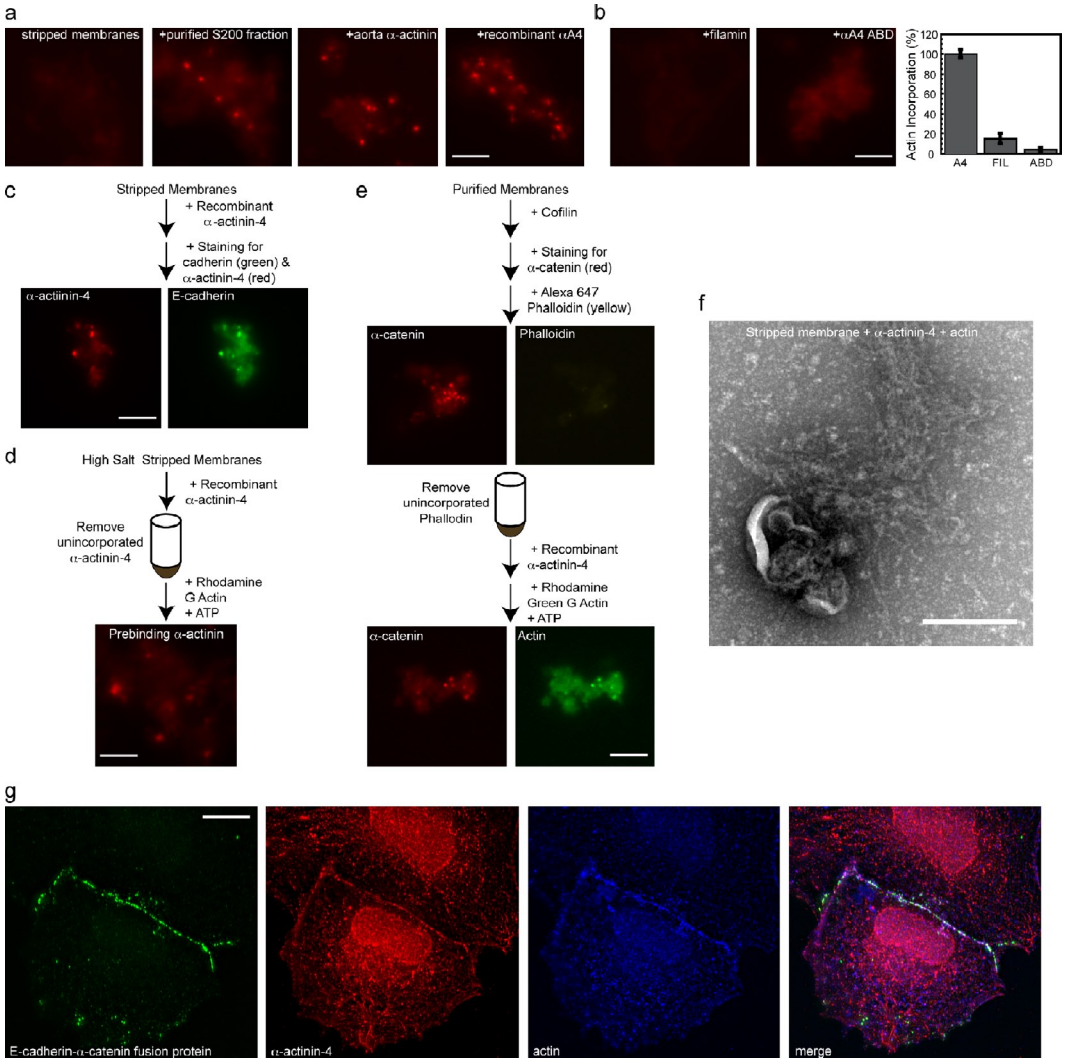

Figure 6. **α-Actinin is an essential factor in actin assembly at E-cadherin junctional complexes.** (a) Actin assembly on stripped membranes can be rescued by from Superdex 200 (S200) fraction B13, α-actinin purified from aorta, or bacterially expressed recombinant α-actinin-4 (αA4). (b) However, filamin (FIL) or the actin-binding domain alone (αA4 ABD) cannot support actin assembly. Error bars represent SEM. $n = 3$. (c) α-Actinin-4 is recruited to E-cadherin foci on stripped membranes. (d) Prebinding α-actinin-4 to membranes rescued actin assembly. (e) α-Actinin-4 can rescue actin assembly on cofilin-treated membranes. (f) Negative-stain EM showing F-actin associated with a stripped membrane fragments after incubation with α-actinin-4 and G-actin. (g) α-Actinin-4 is recruited to cell–cell interactions in CHO cells expressing E-cadherin–α-catenin fusion protein. A projection of five deconvolved optical z slices spanning 1 μm from the apical region of the cells is shown. Bars: (a–c, e, and g) 10 μm; (d) 5 μm; (f) 200 nm.

Actin assembly at adhesion complex requires a salt-extractable factor

As we have an in vitro assay, we can begin to dissect the actin assembly reaction using biochemical reconstitution. Stripping the membranes with 500 mM KCl severely compromised its ability to assemble actin (Fig. 5, a and b). Adding this fraction back to stripped membranes rescued actin assembly (Fig. 5 c). Therefore, an extractable factor can reversibly interact with the membranes to support actin assembly. We used the reconstitution assay to track the extractable factor through six different chromatographic separations, resulting in a 300-fold enrichment of the activity (see Materials and methods; Fig. 5, d and f). The final fraction ran as a symmetrical peak on gel filtration that overlapped with activity (Fig. 5, d and e). The peak activity showed a major band at 100 kD on SDS-PAGE, which was identified by mass spectroscopy as α-actinin-4 as the major component and α-actinin-1 as the minor component (Fig. 5 f).

α-Actinin-4 can rescue actin assembly on stripped membranes

To verify that α-actinin is indeed the salt-extractable activity, we compared the ability of three different preparations of α-actinin to rescue actin assembly on stripped membranes (Fig. 6 a). We found that α-actinin from liver (which expresses α-actinin-1 and -4), aorta (which expresses smooth muscle α-actinin-2), and bacterially expressed recombinant α-actinin-4 all can rescue actin assembly, suggesting that there is no preference for a specific isoform of α-actinin.

α-Actinin is an actin-bundling protein that exists as a dimer and belongs to the calponin homology domain family of actin-binding proteins (Otey and Carpen, 2004). We tested

whether actin assembly requires the cross-linking activity of α-actinin by using a deletion mutant of α-actinin-4 that lacks the dimerization domain (Fig. 6 b). We found that actin binding alone was unable to support assembly at the membrane, suggesting that bundling activity is necessary. To test whether actin bundling is sufficient to support actin assembly, we substituted α-actinin with filamin, a bundling protein that also belongs to the calponin homology family (Feng and Walsh, 2004). We found that filamin was incapable of supporting actin assembly on stripped membranes, suggesting that the requirement for α-actinin is more stringent than simply filament bundling.

α-Actinin-4 marks sites of actin assembly on membranes

To show that α-actinin is localized to sites of actin assembly, we performed the reaction in the presence of rhodamine-labeled α-actinin and rhodamine green–labeled monomeric actin (Fig. S5). Although we observed a complete colocalization of α-actinin and actin, it is unclear whether α-actinin recruitment was a result of copolymerization with actin, as observed by others (Charras et al., 2006), or a result of specific receptors on the membrane. To distinguish between these possibilities, we incubated α-actinin with stripped membranes alone and found that it was recruited to cadherin-enriched foci in the absence of added actin (Fig. 6 c), suggesting that factors already exist on the stripped membranes to act as receptors for α-actinin. Prebinding of α-actinin to stripped membrane and subsequent removal of the unbound proteins were sufficient to rescue actin assembly at junctional foci (Fig. 6 d). Thus, α-actinin appears to have a role in Arp2/3-dependent actin assembly rather than simply organizing the filaments during copolymerization.

To eliminate the possibility that α-actinin binds to residual actin filaments that are left behind after stripping the membranes with high salt, we pretreated the membranes with an actin-depolymerizing factor, cofilin, before performing the actin assembly assay (Fig. 6 e). Pretreatment with cofilin abolished phalloidin binding to membranes without disrupting clustering of α-catenin on the membrane, indicating that these junctional foci are stable in the absence of F-actin. Addition of α-actinin and actin to these pretreated membranes resulted in actin incorporation on α-catenin foci (Fig. 6 e), which is consistent with our conclusion that cadherin–catenin complexes support de novo actin filament formation. α-Actinin has previously been shown to coimmunoprecipitate with the cadherin–catenin complex (Knudsen et al., 1995; Hazan and Norton, 1998; Catimel et al., 2005), which requires α-catenin (Knudsen et al., 1995; Imamura et al., 1999). We expressed a fusion protein of E-cadherin with its cytoplasmic domain fused to α-catenin (Gottardi et al., 2001) in a heterologous cell line, CHO cells. We found that α-actinin-4 and actin were recruited to sites of E-cadherin–α-catenin cell–cell contacts, indicating that the cytoplasmic region of the E-cadherin fusion protein can directly or indirectly link to α-actinin-4 (Fig. 6 f).

If actin is indeed polymerized and assembled on membranes, we should be able to see filaments attached to membranes by negative-stain EM. A reconstitution reaction consisting of stripped membranes, recombinant α-actinin-4, and monomeric actin showed membranes with associating actin filaments (Fig. 6 g). Filaments associated with the membranes were reminiscent of actin architecture associated with the Arp2/3-dependent yeast actin patch (Young et al., 2004), consistent with our observation that actin assembly at cadherin-enriched junctions is Arp2/3 dependent.

α-Actinin-4 localizes to junctional puncta and marks sites of actin assembly in MDCK cells

As the in vitro data demonstrate that α-actinin is required to assemble actin at cadherin-enriched foci, we might expect α-actinin-4 to localize only to actin-positive catenin foci in MDCK cells. Using deconvolution microscopy of polarized MDCK cells, we found that α-actinin-4 indeed colocalized with actin puncta on the lateral membrane (Fig. 7, a and b) but was absent from actin-negative β-catenin puncta (Fig. 7 c). Furthermore, α-actinin-4 was specifically enriched in latrunculin-resistant apical junctional puncta (Fig. 7 d). These α-actinin-4–containing structures would serve as sites of actin assembly after latrunculin washout (Fig. 7 e). In contrast, regions that have β-catenin but lack α-actinin-4 did not show actin recovery. Therefore, consistent with our reconstitution assay, α-actinin-4–containing β-catenin foci faithfully predict sites of actin enrichment and assembly.

Knockdown (KD) of α-actinin-4 retards actin assembly at the apical junction

As the major isoform of α-actinin in the kidney is α-actinin-4 (Kaplan et al., 2000), we designed short hairpin RNAs (shRNAs) to specifically knock down α-actinin-4 in MDCK cells. Three out of four shRNAs tested substantially decreased α-actinin-4 expression (see Materials and methods). We have generated clonal cell lines stably expressing α-actinin-4 shRNAs and showed efficient KD of α-actinin-4 at the protein level (Fig. 8 a). We also performed rescue experiments with human α-actinin-4 that is shRNA resistant (Fig. 8, b–d). We found that KD of α-actinin-4 reduced the amount of apical actin (Fig. 8, b, e, and h), consistent with a major role for α-actinin-4 in junctional actin assembly. However, latrunculin-stable actin puncta still form, implying that other factors are responsible for their stability (Fig. 8, c, f, and i). α-Actinin-4 KD greatly retarded actin recovery after latrunculin washout (Fig. 8, d, g, and j), demonstrating that α-actinin-4 plays a key role in actin assembly at the adherens junction.

α-Actinin-4 point mutation K255E inhibits actin assembly on membranes

Mutations in the α-actinin-4 gene are associated with a common human renal lesion called focal segmental glomerulosclerosis (FSGS; Kaplan et al., 2000). Yet, the molecular mechanisms through which α-actinin-4 mutations translate to FSGS are not known. A disease causing mutation K255E increases the affinity of α-actinin-4 for actin and induces aggregation of cytoplasmic actin filaments (Yao et al., 2004; Weins et al., 2007), but whether these actin aggregates are the causative agent in FSGS is not clear. Therefore, we tested whether K255E α-actinin-4

could support actin assembly at membrane junctional complexes. Whereas both wild-type (WT) and K255E α-actinin-4 could bundle actin filaments (Fig. 9 a) and target to stripped membranes (Fig. 9 b), the K255E mutant protein failed to rescue actin assembly on stripped membranes in the reconstitution assay (Fig. 9 c).

In human, the disease mutation K255E exhibits autosomal-dominant transmission (Kaplan et al., 2000), suggesting that it might behave as a dominant negative. To test this hypothesis, we performed the reconstitution assay using a 1:1 ratio of the WT and K255E. Under these conditions, K255E completely blocked actin assembly (Fig. 9 c), suggesting that the mutant protein acts as a dominant negative to inhibit actin assembly at the junctional complex.

α-Actinin-4 point mutation K255E inhibits actin assembly at adherens junctions in MDCK cells

FSGS patients with α-actinin-4 mutations often are asymptomatic until challenged with other disorders (Shankland, 2006; Lavin et al., 2008). In fact, mice heterozygous for K255E only show mild glomerular ultrastructural changes (Henderson et al., 2008). We found that expression of K255E in MDCK cells did not grossly affect either cell morphology or growth. The mutant protein colocalized with endogenous WT α-actinin-4 at the adherens junction (Fig. 10, a and b) and basal actin structures (Fig. 10 a).

Although K255E is thought to affect actin dynamics in cells (Michaud et al., 2006), we did not see any change in the stability of junctional actin during latrunculin treatment (Fig. 10 c). The amounts of actin were the same at homotypic junctional foci between two cells expressing K255E and at heterotypic junctional foci between a K255E-expressing cell and a nonexpressing cell as well as at homotypic junctional foci between two cells expressing only the endogenous WT α-actinin-4 (Fig. 10 d). However, K255E greatly inhibited actin recovery after latrunculin washout (Fig. 10 e). The levels of actin at junctional foci were inversely correlated with the amounts of K255E present at the junction (Fig. 10 f). There was almost no actin growth at homotypic junctional foci between two cells expressing K255E. Therefore, in agreement with the in vitro reconstitution results, a point mutation in α-actinin-4 associated with FSGS also perturbs actin assembly at cadherin-enriched junctions in vivo.

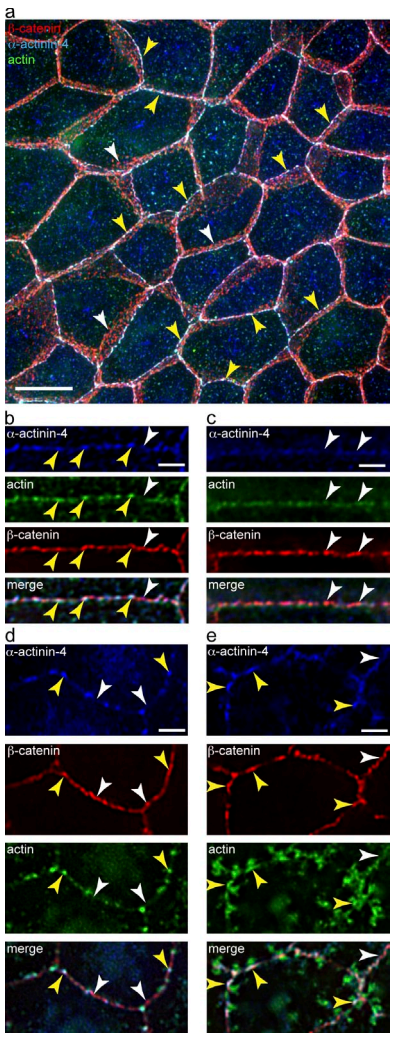

Figure 7. **α-Actinin-4 marks sites of actin assembly in polarized MDCK epithelial cells.** (a) Projection of 25 deconvolved optical z slices spanning the apical 5 µm of cells showing α-actinin-4 colocalization with β-catenin and actin (phalloidin) at the apical junction (yellow arrowheads) but not the lateral membrane (white arrowheads). Bar, 10 µm. (b and c) Single deconvolved optical z slices at the apical (b) and the middle (c) of cells. Yellow arrowheads point to regions where α-actinin-4 (blue), β-catenin (red), and actin (phalloidin; green) are colocalized. White arrowheads point to where α-actinin-4 and actin are missing. (d) A single deconvolved optical z slice after latrunculin treatment. Yellow arrowheads point to areas where α-actinin-4, β-catenin, and actin (phalloidin) are colocalized. White arrowheads point to areas where α-actinin-4 and actin are missing. (e) Single deconvolved optical z slices showing incorporation of actin 15 min after latrunculin washout. Yellow arrowheads point to areas of actin recovery. Areas lacking α-actinin-4 did not show actin recovery (white arrowheads). (b–e) Bars, 2 µm.

Discussion

Cadherin cell–cell adhesion molecules and the actin cytoskeleton are two major determinants of epithelial cell morphology. However, little is known regarding the structural and dynamical organization of actin relative to cadherins in mature epithelial sheets. Using highly polarized cells grown on filters and deconvolution optical sectioning, we distinguished three populations of cadherins on the plasma membrane. Cadherin–catenin complexes concentrated with F-actin near the apical end of the cell as well as the basal end of the cell, although the structural organization of the actin differed at the two sites. Cadherin–catenin complexes along the medial–lateral sides of the cell did not concentrate with F-actin but were simply mixed with the bulk actin cortex. Morphologically distinct cell–cell junctions had been previously described (Drenckhahn and Franz, 1986; Franke, 2009; Franke et al., 2009). Our new analysis demonstrates clear molecular differences in junctional composition and organization within a single polarized cell.

Actin filaments associated with cadherin–catenin foci near the apical surface are more stable than any other actin structures in these cells. Therefore, differences in the structural organization of F-actin as well as filament stability exist along the length of lateral membrane in the apico–basal axis.

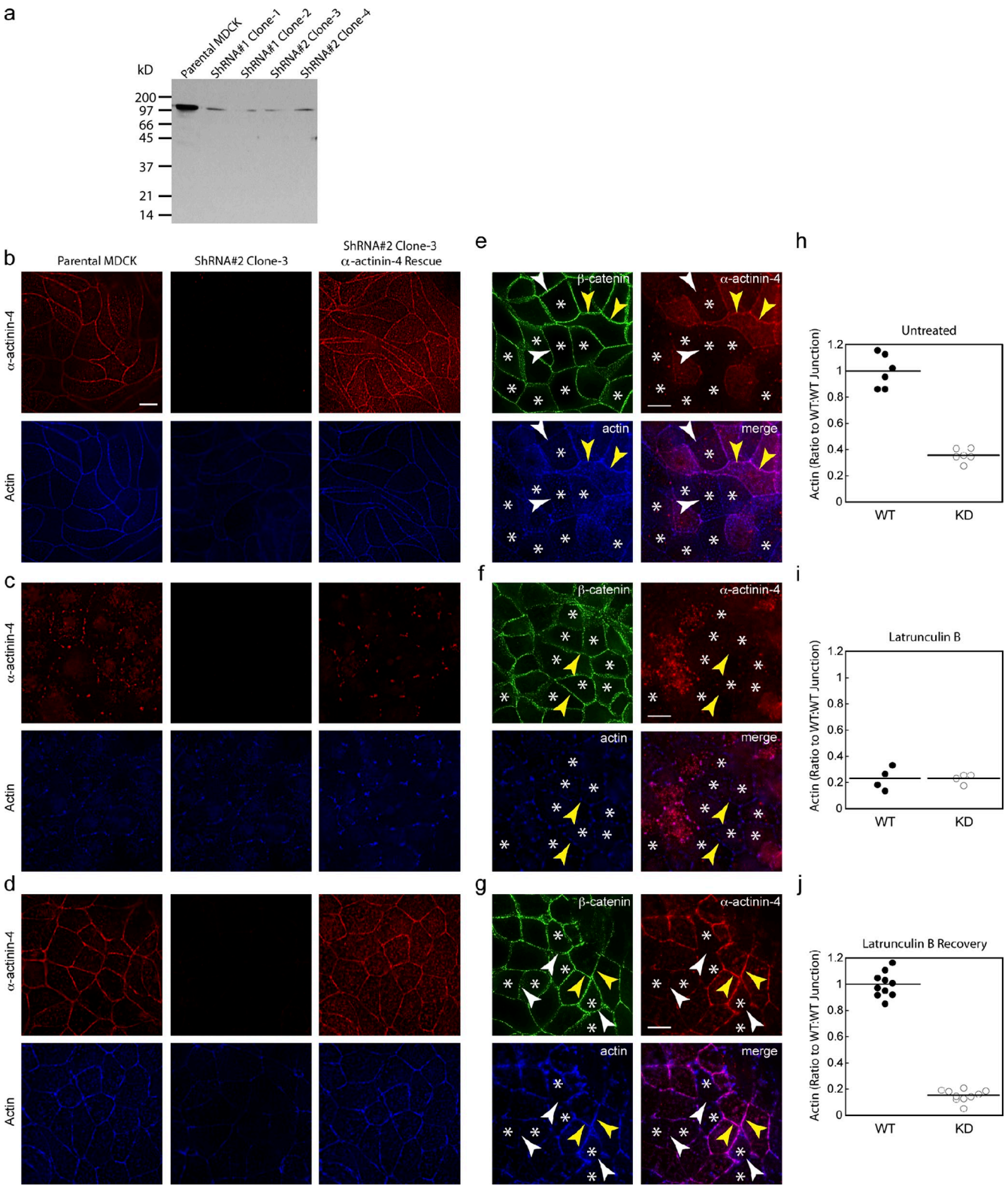

Figure 8. **KD of α-actinin-4 in MDCK cells by shRNA does not alter the overall epithelial morphology but disrupts actin assembly at the apical junction.** (a) Western blot analysis of α-actinin-4 in parental MDCK and clonal cell lines of two different shRNAs against α-actinin-4. Each lane contains an equal amount of total protein. (b) Single deconvolved optical z slices at the apical region of cells showing α-actinin-4 (red) expression correlating with levels of apical actin (phalloidin; blue). (c) Single deconvolved optical z slices at the apical region of latrunculin B–treated cells showing α-actinin-4 levels not correlating with latrunculin-stable actin puncta. (d) Single deconvolved optical z slices at the apical region of cells showing α-actinin-4 expression correlating with actin assembly after latrunculin washout. (e) Projections of 11 deconvolved optical z slices spanning the apical 2 µm of a mixed population of α-actinin-4 KD cells showing normal levels of β-catenin (green). White arrowheads point to junctions with diminished actin between cells with α-actinin-4 KD. (f) Projections of 11 deconvolved optical z slices spanning the apical 2 µm of a mixed population of α-actinin-4 KD cells treated with latrunculin B. Formation of latrunculin-stable actin puncta is unaffected by α-actinin-4 KD. (e and f) Yellow arrowheads point to apical actin puncta formed between cells

These results are inconsistent with the view that treats the actin cytoskeleton along the lateral membrane as one bulk cortex (Rauzi et al., 2008). Our results are more consistent with findings in which different pools of cadherins associate with actin filaments of varying stabilities (Abe and Takeichi, 2008; Cavey et al., 2008; Kovacs et al., 2011).

Identifying the major sites of actin assembly within a cell is important for understanding the spatial organization of the actin cytoskeleton. Monitoring the recovery of a neuronal growth cone's cytoskeleton after treatment with cytochalasin was instrumental in identifying the tip of the advancing lamellipodium as the primary site of actin assembly in the growth cone (Forscher and Smith, 1988). We performed a similar experiment in polarized epithelial cells to identify cadherin-enriched foci near the apical surface as preferred sites of actin assembly upon recovery from latrunculin. In addition, cadherin-enriched foci within plasma membrane sheets were capable of incorporating exogenously added actin monomer in vitro. Therefore, cadherin-enriched foci are preferential sites for actin assembly in mature epithelial cells.

Actin assembly of cadherin-based junction requires the nucleation activity of Arp2/3 in polarized epithelial cells as well as on purified membranes. Although Arp2/3 is classically linked to assembly of highly dynamic actin arrays involved in protrusion of the leading edge of migrating cells or propulsion of internal membranes or pathogens (Machesky and Gould, 1999), our results clearly demonstrated a role for Arp2/3 in a stable latrunculin-resistant pool of actin located at the adherens junction of polarized epithelial cells. These observations underscore the involvement of Arp2/3 in different actin structures with distinct dynamics and stabilities. Previous studies had demonstrated that Arp2/3 coimmunoprecipitates with the cadherin–catenin complex (Kovacs et al., 2002) and interacts with several known adherens junctional proteins, including vinculin and neuronal Wiskott–Aldrich Syndrome protein (DeMali et al., 2002; Weaver et al., 2002). Our results are consistent with Arp2/3 having an essential role in actin assembly at cadherin-mediated contacts (Kovacs et al., 2002, 2011). However, the precise mechanisms through which Arp2/3 is recruited to and activated at that site remain mysterious and might possibly occur through noncanonical pathways distinct from Arp2/3 activation described for other systems (Kovacs et al., 2011). Future directions will be to understand how Arp2/3 is recruited to cell–cell contacts to organize actin in epithelial cells.

We established a new in vitro system that reconstitutes actin assembly at cadherin-enriched membrane foci and used it to identify α-actinin-4 as a factor necessary for actin assembly at these sites. Whereas α-actinin binds and bundles F-actin, junctional foci could not capture preformed actin filaments in vitro. Rather, α-actinin–dependent actin assembly required

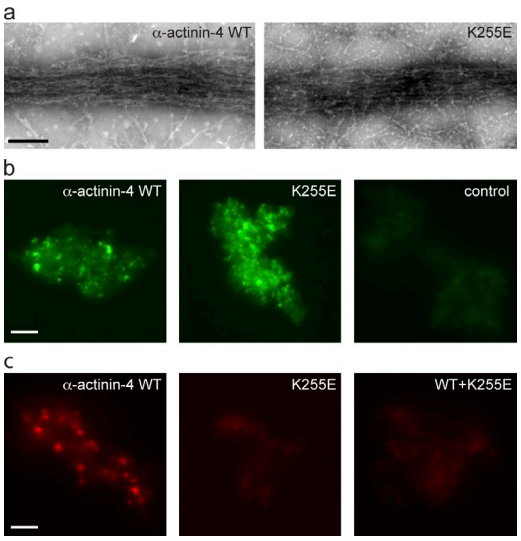

Figure 9. **FSGS disease mutation K255E inhibits actin assembly on membranes.** (a) Negative-stain EM showing bundling of actin filaments by WT and K255E α-actinin-4. Bar, 200 nm. (b) WT and K255E are recruited to stripped membranes. (c) K255E did not support actin assembly on stripped membranes and inhibited the activity of WT α-actinin-4. (b and c) Bar, 2 µm.

G-actin and Arp2/3-dependent actin nucleation. Perhaps actin assembly at cadherin junctions requires tight coupling of actin polymerization and bundling activity, as has been shown in *Listeria monocytogenes* comet tails (Brieher et al., 2004). Focusing actin polymerization at the junction using localized nucleation factors such as Arp2/3 might facilitate subsequent capture of filaments by α-actinin localized to the junction. However, a point mutation of α-actinin K255E that binds to F-actin with a higher affinity than WT (Weins et al., 2007) fails to support actin assembly. Either the biochemical and structural requirements for capturing filaments at junctions are stringent or α-actinin contributes to actin assembly in ways additional to bundling F-actin alone. Our reconstituted system provides a new approach to elucidate how α-actinin and Arp2/3 collaborate to assemble actin at cadherin-enriched junctions.

α-Actinin has previously been shown to coimmunoprecipitate with the cadherin–catenin complex (Knudsen et al., 1995; Hazan and Norton, 1998; Catimel et al., 2005), which requires α-catenin (Knudsen et al., 1995; Imamura et al., 1999). Our results assign a functional significance to these classical observations. What remains to be determined is the precise molecular connection between α-actinin and the cadherin–catenin complex. Attempts to link α-actinin to the cadherin–catenin complex in vitro have been unsuccessful (Yamada et al., 2005). Nevertheless, a cadherin–α-catenin fusion protein can recruit α-actinin-4 and actin to cell–cell contacts (Imamura et al., 1999; this study). The combined work implies that factors

with α-actinin-4 KD cells (asterisks). (g) Projections of 11 deconvolved optical z slices spanning the apical 2 µm of a mixed population of α-actinin-4 KD cells after latrunculin washout. White arrowheads point to junctions with diminished actin recovery. Yellow arrowheads point to normal actin recovery between cells with normal levels of actinin-4. Asterisks are the same as described in e and f. (b–g) Bars, 10 µm. (h) Quantitation of actin (phalloidin) at junctions between WT/WT and KD/KD cells. (i) Quantitation of actin (phalloidin) at junctions between WT/WT and KD/KD cells treated with latrunculin B. (j) Quantitation of actin (phalloidin) at junctions between WT/WT and KD/KD cells 30 min after latrunculin B washout. (h–j) Each line represents the mean value of all the individual data points in that group.

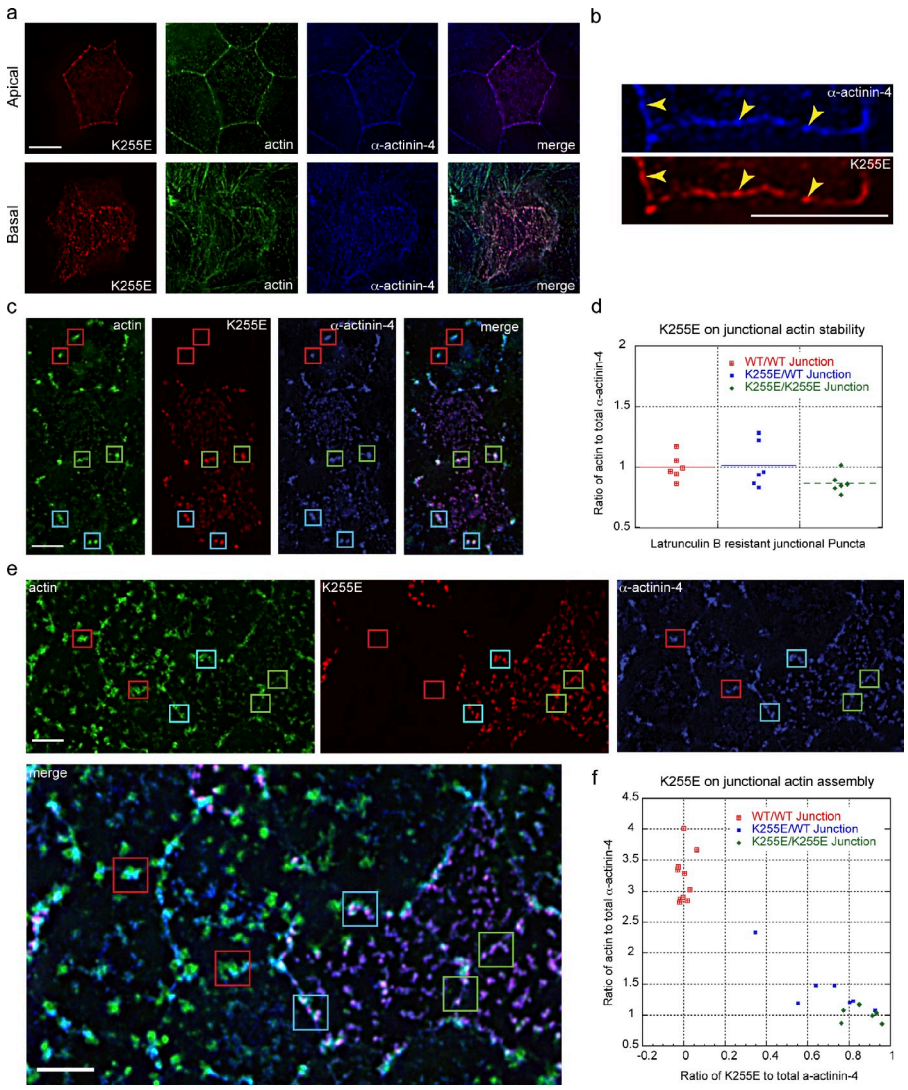

Figure 10. **FSGS disease mutation K255E inhibits actin assembly at cell junctions of epithelial cells.** (a) FSGS disease mutation K255E colocalizes with endogenous α-actinin-4 at apical junction and basal sarcomeric structures in polarized MDCK cells. Single deconvolved optical z slices at the apical and basal regions of cells are shown. (b) Single deconvolved optical z slices at the apical region of cells. Yellow arrowheads point to colocalization of α-actinin-4 (blue), K255E (red), and actin (phalloidin; green). (a and b) Bars, 10 µm. (c) Latrunculin-stable actin puncta in homotypic K255E/K255E junctions (green squares), homotypic α-actinin-4 WT/WT junctions (red squares), or heterotypic K255E/WT junctions (blue squares). Bar, 5 µm. (d) Actin stability is independent of K255E levels. Quantitation of actin (phalloidin) to total α-actinin-4 levels in latrunculin-stable puncta. Solid lines represent the means of the data points. (e) Actin assembly at junctional puncta in homotypic K255E/K255E junctions, homotypic WT/WT junctions, or heterotypic K255E/WT junctions 15 min after latrunculin washout. Bars, 5 µm. (f) The amount of actin recovery is inversely proportional to the amount of K255E in the puncta. Quantitation of actin recovery 15 min after latrunculin washout is shown. The ratio of actin (phalloidin) to total α-actinin-4 is plotted as a function of the ratio of K255E to total α-actinin-4.

in addition to α-catenin are required to recruit α-actinin and actin. An important question will be to understand how α-actinin coordinates with other junctional components to support actin assembly at cell–cell contacts.

Human mutations in the α-actinin-4 gene are linked to a common human renal lesion, FSGS (Kaplan et al., 2000). Although the precise mechanism is not known, it has been postulated that the disease causing mutation K255E disrupts actin dynamics by both gain-of-function and loss-of-function mechanisms (Yao et al., 2004). In support of the loss-of-function mechanism, we found that K255E failed to rescue actin assembly on membrane foci in a membrane reconstitution assay. Furthermore, K255E inhibited actin assembly in the presence of WT α-actinin-4 both in vitro and in vivo. As the human K255E mutation is associated with an autosomal-dominant form of FSGS (Kaplan et al., 2000), we proposed that K255E plays a role not only as a loss-of-function mutant but also as a dominant negative to the WT α-actinin-4. Although specialized junctions such as the adherens junctions appear to be more stable than other cadherin-mediated cell–cell contacts, some degree of actin turnover is expected that would require new actin assembly to maintain a steady state. Mutations in α-actinin-4, otherwise silent during development, could progressively compromise junctional actin organization over time and when challenged with other genetic defects and environmental insults.

Materials and methods

Antibodies and reagents

Antibodies to α- and β-catenin were provided by B. Gumbiner (University of Virginia, Charlottesville, VA). Antibodies to β-catenin (catalog no. 7963), E-cadherin (catalog no. 21791), Arp2 (catalog no. 10125), Arp3 (catalog nos. 10132 and 136279), PI3K p110-γ (catalog no. 7177), and S-tag (for detection of K255E; catalog no. 101595) were purchased from Santa Cruz Biotechnology, Inc. Antibodies to formin-1 (catalog no. 44110002) were purchased from Novus Biologicals. Antibodies to α-actinin-4 were raised in house against a synthetic N-terminal peptide, NQSYQYGPSSAGNGAGC, coupled to KLH. Secondary antibodies were obtained from Bio-Rad Laboratories (HRP anti–mouse and HRP anti–rabbit) and Invitrogen (FITC and Cy3 anti–mouse and FITC and Cy3 anti–rabbit). Rhodamine, rhodamine green, latrunculin B, cytochalasin D, FITC-phalloidin, TRITC-phalloidin, blebbistatin, CK-636, CK-548, and SMIFH2 were purchased from Sigma-Aldrich. Stock solutions of latrunculin B (5 mM), cytochalasin D (2 mM), blebbistatin (5 mM), CK-548 (20 mM), CK-636 (20 mM), and SMIFH2 (100 mM) were prepared in DMSO. Alexa Fluor 647 and 647–phalloidin were purchased from Invitrogen. Leupeptin, Pefabloc, E-64, antipain, aprotinin, bestatin, and calpain inhibitors I and II were purchased

from A.G. Scientific, Inc. Polyethyleneimine was purchased form Sigma-Aldrich. Protein concentrations were determined by the detergent-compatible protein assay (Bio-Rad Laboratories).

DNA constructs

α-Actinin-4 WT and K255E cDNAs were provided by M. Pollak (Brigham and Women's Hospital and Harvard Medical School, Boston, MA). The coding sequence of the α-actinin-4 full-length actin-binding domain (1–270) and full-length K255E was subcloned into EcoR1 and Xho1 sites in the bacterial expression vector pET30a+ (EMD) for expression in Rosetta cells (EMD). Full-length α-actinin-4 WT and K255E mutant was subcloned into EcoR1 and Xho1 sites of the G418-selectable mammalian expression vector pNTAPB (Agilent Technologies) with a streptavidin-binding peptide tag at the N terminus for expression in MDCK cells. shRNAs for α-actinin-4 (5′-ACACAGATAGAGAACATCGACGAGGACTT-3′, 5′-CTGTCAACCAGGAGAATGAACACCTCATG-3′, and 5′-AGGTCCTG-TTCCTCTGACTCGGTATCTAT-3′) were synthesized and subcloned into blasticidin-selectable pGFP-B-RS vector (OriGene). The E-cadherin–α-catenin fusion construct was provided by C. Gottardi (Northwestern Medical School, Chicago, IL).

Protein purification

For expression of recombinant 6-His–tagged α-actinin-4, actin-binding domain, and K255E, Rosetta cells were induced with 500 µM isopropyl β-D-1-thiogalactopyranoside for 8 h at 25°C. Cells were centrifuged at 6,000 *g* for 15 min and resuspended in 20 mM NaCl and 20 mM Hepes, pH 7.8, in the presence of 5 mg/ml lysozyme. After a freeze-thaw cycle, lysed cells were centrifuged at 20,000 *g* for 30 min. The supernatant was loaded onto a nickel column (QIAGEN). The column was washed with 20-bed columns of 500 mM NaCl, 25 mM imidazole, and 20 mM Hepes, pH 7.8. The recombinant proteins were eluted with 10-bed volumes of 500 mM NaCl, 500 mM imidazole, and 20 mM Hepes, pH 7.8. Full-length proteins were concentrated using Centricon (Millipore) and purified by gel filtration in 150 NaCl, 20 mM Hepes, and 10 mM β-mercaptoethanol. Recombinant CapZ (Maun et al., 1996), actin (Brieher et al., 2004), aortic α-actinin (Brieher et al., 2004), filamin (Brieher et al., 2004), and profilin were purified as previously described (Brieher et al., 2006). The profilin–actin complex was allowed to form overnight at a 2:1 profilin/actin ratio. Actin and aorta α-actinin were labeled with fluorophores as previously described (Brieher et al., 2004). In brief, F-actin was labeled on lysine residues using two *N*-hydroxysuccinimide–activated fluorophores for every actin molecule for 1 h at room temperature. Filaments were then pelleted at 100,000 *g* for 30 min, resuspended in G buffer, and dialyzed exhaustively against G buffer. This procedure typically labeled actin to 50–80%. α-Actinin was labeled on cysteine using maleimide-activated fluorophores at a ratio of five fluorophores for every α-actinin at room temperature for 1 h. Labeled proteins were separated from free dyes by gel filtration using Superdex 200 (GE Healthcare).

Cell culture

MDCK cells were maintained in MEM/Earle's balanced salt solution (EBSS) supplemented with 25 mM Hepes and 10% FBS. For transfection, MDCK cells were incubated in Opti-MEM (Invitrogen) with a 1:1 mixture of DNA/polyethyleimine and selected for 10 d using G418 or blasticidin.

In vitro and in vivo actin incorporation

For in vitro assays, MDCK cells grown on Costar transwells (Corning) for 7 d were either treated with 10 µM latrunculin or DMSO in normal growth media for 2 h before use. Cells were rinsed twice in EBSS with 20 mM Hepes, pH 7.5, at room temperature. Cells were permeabilized in the presence of 0.5 µM fluorescently labeled monomeric actin in saponin buffer (0.2 mg/ml saponin, 100 mM KCl, 2 mM $MgCl_2$, 2 mM EGTA, and 20 mM Hepes, pH 7.8) at room temperature for 10 min. The cells were rinsed quickly in saponin buffer and fixed with 1% formaldehyde in saponin buffer at 4°C for 60 min and processed for immunofluorescence.

For in vivo assays, MDCK cells grown on Costar transwells for 7 d were treated with 10 µM latrunculin in normal growth media for 2 h and then either processed for immunofluorescence or rinsed in fresh media in the presence or the absence of CK-548/CK-636 or SMIFH2 to initiate actin recovery. Cells were subsequently processed for immunofluorescence at various time points.

Immunofluorescence of cells

MDCK cells grown on Transwell-Clear (Corning) for 10 d were rinsed twice in EBSS and fixed in 1% formaldehyde/150 mM NaCl/20 mM Hepes, pH 7.8, at 4°C for 90 min. The reaction was quenched with 50 mM Tris in staining buffer (0.1% Triton X-100/100 mM NaCl/20 mM Hepes, pH 7.8) for 1 h. After rinsing in staining buffer, the cells were incubated with primary antibodies in staining buffer overnight. After rinsing in staining buffer three times, the cells were incubated in secondary antibodies for 90 min. The cells were rinsed again three times and poststain fixed with 1% formaldehyde in staining buffer. Finally, the cells were incubated with fluorescently labeled phalloidin for 60 min. Transwell filters were excised and mounted on glass slides using ProLong Gold antifade (Invitrogen).

Optical z slices in 200-nm steps were collected with a microscope (1X71; Olympus) attached to a 1K × 1K charge-coupled device camera using a 60× objective (NA 1.42) with a 1.6× auxiliary magnification. All images were deconvolved using DeltaVision software (Applied Precision). Z stack projections were generated from deconvolved slices using the maximum intensity criteria. Composite images were generated using ImageJ software (National Institutes of Health). Quantitation of actin puncta intensity was performed in ImageJ using unprocessed original images. A defined area (120 × 120 pixels) was used to compare the signal intensity of actin (phalloidin), K255E (immunofluorescence using S-tag antibodies), and α-actinin-4 (immunofluorescence using N terminus α-actinin-4 antibodies). The measured intensities were subtracted from background (cytoplasm) before being used for calculating the intensity ratios. For figure generation, images were cropped, contrasted, and scaled using Photoshop software (Adobe) before importing into Illustrator (Adobe).

Actin assembly and reconstitution assays

Actin assembly assays were performed in actin assembly buffer (50 mM KCl, 2 mM EGTA, 2 mM $MgCl_2$, and 100 mM Hepes, pH 7.8) supplemented with 2 mM buffered ATP, pH 8. In brief, a 20-µL reaction consists of ∼15 µg of total proteins from membrane fraction and 0.5 µM fluorescently labeled monomeric actin. For assay with filamentous actin, fluorescently labeled monomeric actins were allowed to polymerize overnight before use. For reconstitution assays, purified membranes were stripped with 500 mM NaCl, 2 mM $MgCl_2$, 2 mM EGTA, 20 mM Hepes, pH 7.8, and 10 mM DTT on ice for 1 h. Stripped membranes were collected by centrifugation at 10,000 *g* for 10 min. The supernatant was dialyzed against actin assembly buffer and used for reconstitution assay. A 20-µL reconstitution assay consists of ∼8 µg of total protein from stripped membranes, 0.5 µM fluorescently labeled actin, and test fractions with protein concentrations ranging from 0.1 µg to several micrograms. The reactions were imaged using an Axio Imager with the Colibri illumination system (Carl Zeiss) using a 63× objective (NA 1.4) attached to a 1K × 1K charge-coupled device camera (ORCA-ER; Hamamatsu Photonics).

Immunofluorescence of membranes

Actin assembly reactions were allowed to carry out for 3 h before incubation with primary antibodies in the presence of 0.1% Triton X-100. The membranes were spun through a 20% sucrose cushion and resuspended in 0.1% Triton X-100 in assay buffer. The membranes were incubated with secondary antibodies for 2 h, spun through a 20% sucrose cushion, and resuspended in 0.1% Triton X-100 in assay buffer. For immunofluorescence of α-actinin-4 on membranes, the WT and K255E proteins were allowed to prebind to stripped membranes for 1 h on ice and were processed for immunofluorescence as previously described. Stained membranes were imaged using the Axio Imager as previously described.

Quantitating actin assembly on membranes

Actin incorporation on membranes was measured by fluorometry. The actin assembly reactions were initiated by the addition of ATP and rhodamine-labeled monomeric actin. The reactions were stopped at varies time points by centrifuging the membranes through a 20% sucrose cushion. Membrane pellets were solubilized in 1% SDS, and fluorescence was measured in a fluorometer with excitation at 542 nm and emission at 568 nm. The readings were subtracted from a background reading of membrane and ATP without actin. The amount of actin incorporation was calculated from the reading of a known quantity of rhodamine-labeled actin. For F-actin binding, G-actin was prepolymerized for 2 h before use. The readings were subtracted from the background reading in the presence of latrunculin. For drug inhibition assays, cytochalasin D and latrunculin B were added to the membranes before initiation of actin assembly reactions. For profilin–actin assay, preformed profilin–rhodamine-labeled actin complex (at a ratio of two profilins to one actin) was added instead of actin. For CapZ experiments, CapZ was added to the membranes before the initiation of actin assembly reactions. For CapZ prebinding, 100 nM CapZ was added to the membranes for 30 min before spinning through 20% sucrose. The CapZ-treated membranes were resuspended in assembly buffer, and the actin assembly reactions were initiated as previously described.

Cell homogenization and liver membrane purification

MDCK and T84 cell homogenates were prepared as follows. Cells were rinsed and hypoosmotically shocked on dish in 10 mM Hepes, pH 8.5, for 60 min at 4°C. Cells were scraped and homogenized on ice through a 25-guage needle in 10 mM Hepes, pH 8.5, in the presence of 10 mM DTT and protease inhibitors (10 µg/ml leupeptin, 1 mg/ml Pefabloc, 10 µg/ml E-64, 2 µg/ml antipain, 2 µg/ml aprotinin, 50 µg/ml bestatin, 20 µg/ml calpain inhibitor I, and 10 µg/ml calpain inhibitor II).

Liver homogenate was prepared as follows. Frozen rat livers (Pel-Freez Biologicals) were thawed in 2 vol of 10 mM Hepes, pH 8.5/10 mM DTT. Protease inhibitors (see above) were added, and the livers were briefly blended in a blender (5 × 15 s; Waring). The liver slush was filtered through four layers of cheesecloth to obtain the total liver homogenate. Liver membrane fractionation was performed using sequential centrifugation and equilibrium density sucrose gradient (Fig. S3). Altogether, eight different membrane fractions were isolated, and only two have actin assembly activity under the assay conditions used. The majority of actin assembly activity was in a single membrane fraction. This membrane fraction was prepared as follows. Total liver homogenate was centrifuged at 1,000 *g* for 30 min. The pellet was homogenized in 10 mM Hepes, pH 8.5/10 mM DTT in a Dounce homogenizer and centrifuged at 100 *g* for 30 min. The supernatant was collected and centrifuged at 1,000 *g* for 30 min. This membrane pellet contains the majority of actin assembly activity and is used as the purified membrane fraction in all experiments.

Fractionation of high-salt–extractable factor

Reconstitution assays (see Actin assembly and reconstitution assays section) were used to track the fractions that could rescue actin assembly on stripped membranes. High-salt extracts were obtained by stripping membranes with 500 mM NaCl, 2 mM $MgCl_2$, 2 mM EGTA, 20 mM Hepes, pH 7.8, and 10 mM DTT on ice for 1 h. The membranes were removed by centrifugation at 10,000 *g* for 30 min. The supernatant was dialyzed against 10 mM Hepes, pH 7.8, and 10 mM β-mercaptoethanol overnight at 4°C and subsequently centrifuged at 10,000 *g* for 30 min. This clarified supernatant was used for purification of actin assembly activity using a fast protein liquid chromatography system (AKTA; GE Healthcare). The supernatant was loaded on to a HiTrap S HP column (GE Healthcare). The S flowthrough contained most of the actin assembly activity and was loaded onto a HiTrap Blue HP column. The Blue flowthrough contained most of the activity and was loaded onto a HiTrap Heparin HP column. The HP flowthrough contained most of the activity and was loaded onto a HiTrap Q HP column. Most of the activity was bound to Q HP and was eluted with a linear gradient of 0–500 mM NaCl, 10 mM Hepes, pH 7.8, and 10 mM β-mercaptoethanol. The fractions were desalted against the actin assembly buffer using Sephadex G-25 (GE Healthcare) spin columns before testing in the reconstitution assay. Peak activity was found between 27.8 and 31.5 mS/cm. The fractions were pooled, dialyzed against 10 mM Hepes, pH 7.8, and 10 mM β-mercaptoethanol overnight at 4°C and subsequently centrifuged at 10,000 *g* for 30 min. The supernatant was loaded on to a Tricorn Source Q column (GE Healthcare) and eluted with a linear gradient of 0–500 mM NaCl, 10 mM Hepes, pH 7.8, and 10 mM β-mercaptoethanol. The fractions were desalted using Sephadex G-25 spin columns before testing in the reconstitution assay. Fractions eluted at 24.2–25.1 mS had peak actin assembly activity and were concentrated using a Centricon filter unit. The concentrate was centrifuged at 10,000 *g* for 30 min and loaded onto a Superdex 200 column. Two major and several minor symmetrical peaks were resolved in the Superdex column, and only one peak has the actin assembly activity.

EM

MDCK cells grown on Transwell-Clear were processed for EM as previously described (Tang, 2006). In brief, cells/transwells were chilled at 4°C for 6 h before fixation with 3.75% glutaraldehyde, 150 mM NaCl, and 20 mM Hepes, pH 7.5, at 4°C for 18 h. The fixation reaction was quenched with 50 mM glycine and 150 mM Hepes, pH 7.5, on ice for 1 h. Cells/transwells were rinsed in ice-cold distilled water three times, secondary fixed with 1% osmium tetroxide/1.5% potassium ferrocyanide for 2 h on ice, rinsed four times in ice-cold distilled water, en bloc stained with freshly prepared and filtered 2% uranyl acetate in distilled water on ice for 2 h, and rinsed four times in ice-cold distilled water. Cells/transwells were dehydrated with sequential 5-min incubations in 50, 75, 95, 100, 100, and 100% ethanol at room temperature. Epon-Araldite (EMbed 812) was added to transwells and allowed to polymerize at 60°C for 48 h. Ultrathin sections were cut using a microtome (UltraCut S; Reichert), layered onto carbon-coated copper grids, and stained with freshly made/filtered 2% lead citrate. Images were collected with a microscope (1200EX; JOEL, Ltd.) at 60 kV. For actin-negative stain, recombinant α-actinin-4 and K255E proteins were copolymerized with actin for 2 h in actin assembly buffer. The samples were put onto glow-discharged carbon-coated grids for 5 min, washed three times with assembly buffer, and stained with 2% uranyl acetate. For membrane-negative stain, stripped membranes were prebound with recombinant α-actinin-4 for 60 min before initiation of actin assembly by adding ATP and monomeric actin. The reaction was allowed to continue for 60 min before put onto on glow-discharged carbon-coated grids for 5 min, washed three times with assembly buffer, and stained with 2% uranyl acetate. Images were collected with a microscope (JEOL 1200EX) at 200 kV using a 2K × 2K charge-coupled device camera (UltraScan; Gatan, Inc.).

Online supplemental material

Fig. S1 shows incorporation of fluorescently labeled actin at apical, lateral, and basal regions of saponin-permeabilized cells. Fig. S2 shows relative contribution of actin nucleators, Arp2/3, and formin in MDCK cells. Fig. S3 shows immunofluorescence staining of β-catenin and formin-1. Fig. S4 shows fractionation of liver membranes. Fig. S5 shows that actin incorporation at the membrane is saturable. Online supplemental material is available at http://www.jcb.org/cgi/content/full/jcb.201103116/DC1.

We thank Dr. Barry Gumbiner for α- and β-catenin antibodies. We thank Dr. Martin Pollak for α-actinin-4 WT and K255E cDNAs. We thank Dr. Cara Gottardi for cDNA of human E-cadherin–α-catenin fusion protein. We thank Krista Angileri for assistance with molecular biology. EM was carried out in part in the University of Illinois Frederick Seitz Materials Research Laboratory central facilities.

This work is funded by a grant from the March of Dimes.

Submitted: 22 March 2011
Accepted: 6 December 2011

References

Abe, K., and M. Takeichi. 2008. EPLIN mediates linkage of the cadherin catenin complex to F-actin and stabilizes the circumferential actin belt. *Proc. Natl. Acad. Sci. USA*. 105:13–19. http://dx.doi.org/10.1073/pnas.0710504105

Adams, C.L., Y.T. Chen, S.J. Smith, and W.J. Nelson. 1998. Mechanisms of epithelial cell–cell adhesion and cell compaction revealed by high-resolution tracking of E-cadherin–green fluorescent protein. *J. Cell Biol.* 142:1105–1119. http://dx.doi.org/10.1083/jcb.142.4.1105

Angres, B., A. Barth, and W.J. Nelson. 1996. Mechanism for transition from initial to stable cell-cell adhesion: Kinetic analysis of E-cadherin-mediated adhesion using a quantitative adhesion assay. *J. Cell Biol.* 134:549–557. http://dx.doi.org/10.1083/jcb.134.2.549

Bershadsky, A. 2004. Magic touch: How does cell-cell adhesion trigger actin assembly? *Trends Cell Biol.* 14:589–593. http://dx.doi.org/10.1016/j.tcb.2004.09.009

Brieher, W.M., M. Coughlin, and T.J. Mitchison. 2004. Fascin-mediated propulsion of *Listeria monocytogenes* independent of frequent nucleation by the Arp2/3 complex. *J. Cell Biol.* 165:233–242. http://dx.doi.org/10.1083/jcb.200311040

Brieher, W.M., H.Y. Kueh, B.A. Ballif, and T.J. Mitchison. 2006. Rapid actin monomer–insensitive depolymerization of *Listeria* actin comet tails by cofilin, coronin, and Aip1. *J. Cell Biol.* 175:315–324. http://dx.doi.org/10.1083/jcb.200603149

Cao, L.G., D.J. Fishkind, and Y.L. Wang. 1993. Localization and dynamics of nonfilamentous actin in cultured cells. *J. Cell Biol.* 123:173–181. http://dx.doi.org/10.1083/jcb.123.1.173

Carramusa, L., C. Ballestrem, Y. Zilberman, and A.D. Bershadsky. 2007. Mammalian diaphanous-related formin Dia1 controls the organization of E-cadherin-mediated cell-cell junctions. *J. Cell Sci.* 120:3870–3882. http://dx.doi.org/10.1242/jcs.014365

Catimel, B., J. Rothacker, J. Catimel, M. Faux, J. Ross, L. Connolly, A. Clippingdale, A.W. Burgess, and E. Nice. 2005. Biosensor-based microaffinity purification for the proteomic analysis of protein complexes. *J. Proteome Res.* 4:1646–1656. http://dx.doi.org/10.1021/pr050132x

Cavey, M., M. Rauzi, P.F. Lenne, and T. Lecuit. 2008. A two-tiered mechanism for stabilization and immobilization of E-cadherin. *Nature*. 453:751–756. http://dx.doi.org/10.1038/nature06953

Charras, G.T., C.K. Hu, M. Coughlin, and T.J. Mitchison. 2006. Reassembly of contractile actin cortex in cell blebs. *J. Cell Biol.* 175:477–490. http://dx.doi.org/10.1083/jcb.200602085

Chu, Y.S., W.A. Thomas, O. Eder, F. Pincet, E. Perez, J.P. Thiery, and S. Dufour. 2004. Force measurements in E-cadherin–mediated cell doublets reveal rapid adhesion strengthened by actin cytoskeleton remodeling through Rac and Cdc42. *J. Cell Biol.* 167:1183–1194. http://dx.doi.org/10.1083/jcb.200403043

DeMali, K.A., C.A. Barlow, and K. Burridge. 2002. Recruitment of the Arp2/3 complex to vinculin: Coupling membrane protrusion to matrix adhesion. *J. Cell Biol.* 159:881–891. http://dx.doi.org/10.1083/jcb.200206043

Drenckhahn, D., and H. Franz. 1986. Identification of actin-, alpha-actinin-, and vinculin-containing plaques at the lateral membrane of epithelial cells. *J. Cell Biol.* 102:1843–1852. http://dx.doi.org/10.1083/jcb.102.5.1843

Feng, Y., and C.A. Walsh. 2004. The many faces of filamin: A versatile molecular scaffold for cell motility and signalling. *Nat. Cell Biol.* 6:1034–1038. http://dx.doi.org/10.1038/ncb1104-1034

Flanagan, M.D., and S. Lin. 1980. Cytochalasins block actin filament elongation by binding to high affinity sites associated with F-actin. *J. Biol. Chem.* 255:835–838.

Forscher, P., and S.J. Smith. 1988. Actions of cytochalasins on the organization of actin filaments and microtubules in a neuronal growth cone. *J. Cell Biol.* 107:1505–1516. http://dx.doi.org/10.1083/jcb.107.4.1505

Franke, W.W. 2009. Discovering the molecular components of intercellular junctions—a historical view. *Cold Spring Harb. Perspect. Biol.* 1:a003061. http://dx.doi.org/10.1101/cshperspect.a003061

Franke, W.W., S. Rickelt, M. Barth, and S. Pieperhoff. 2009. The junctions that don't fit the scheme: Special symmetrical cell-cell junctions of their own kind. *Cell Tissue Res.* 338:1–17. http://dx.doi.org/10.1007/s00441-009-0849-z

Gottardi, C.J., E. Wong, and B.M. Gumbiner. 2001. E-cadherin suppresses cellular transformation by inhibiting β-catenin signaling in an adhesion-independent manner. *J. Cell Biol.* 153:1049–1060. http://dx.doi.org/10.1083/jcb.153.5.1049

Gumbiner, B.M. 1996. Cell adhesion: The molecular basis of tissue architecture and morphogenesis. *Cell*. 84:345–357. http://dx.doi.org/10.1016/S0092-8674(00)81279-9

Gumbiner, B.M. 2005. Regulation of cadherin-mediated adhesion in morphogenesis. *Nat. Rev. Mol. Cell Biol.* 6:622–634. http://dx.doi.org/10.1038/nrm1699

Hammerschmidt, M., and D. Wedlich. 2008. Regulated adhesion as a driving force of gastrulation movements. *Development*. 135:3625–3641. http://dx.doi.org/10.1242/dev.015701

Hazan, R.B., and L. Norton. 1998. The epidermal growth factor receptor modulates the interaction of E-cadherin with the actin cytoskeleton. *J. Biol. Chem.* 273:9078–9084. http://dx.doi.org/10.1074/jbc.273.15.9078

Hemmings, L., P.A. Kuhlman, and D.R. Critchley. 1992. Analysis of the actin-binding domain of alpha-actinin by mutagenesis and demonstration that dystrophin contains a functionally homologous domain. *J. Cell Biol.* 116:1369–1380. http://dx.doi.org/10.1083/jcb.116.6.1369

Henderson, J.M., S. Al-Waheeb, A. Weins, S.V. Dandapani, and M.R. Pollak. 2008. Mice with altered alpha-actinin-4 expression have distinct morphologic patterns of glomerular disease. *Kidney Int.* 73:741–750. http://dx.doi.org/10.1038/sj.ki.5002751

Imamura, Y., M. Itoh, Y. Maeno, S. Tsukita, and A. Nagafuchi. 1999. Functional domains of α-catenin required for the strong state of cadherin-based cell adhesion. *J. Cell Biol.* 144:1311–1322. http://dx.doi.org/10.1083/jcb.144.6.1311

Itoh, M., A. Nagafuchi, S. Moroi, and S. Tsukita. 1997. Involvement of ZO-1 in cadherin-based cell adhesion through its direct binding to α catenin and actin filaments. *J. Cell Biol.* 138:181–192. http://dx.doi.org/10.1083/jcb.138.1.181

Kang, F., D.L. Purich, and F.S. Southwick. 1999. Profilin promotes barbed-end actin filament assembly without lowering the critical concentration. *J. Biol. Chem.* 274:36963–36972. http://dx.doi.org/10.1074/jbc.274.52.36963

Kaplan, J.M., S.H. Kim, K.N. North, H. Rennke, L.A. Correia, H.Q. Tong, B.J. Mathis, J.C. Rodríguez-Pérez, P.G. Allen, A.H. Beggs, and M.R. Pollak. 2000. Mutations in ACTN4, encoding alpha-actinin-4, cause familial focal segmental glomerulosclerosis. *Nat. Genet.* 24:251–256. http://dx.doi.org/10.1038/73456

Knudsen, K.A., A.P. Soler, K.R. Johnson, and M.J. Wheelock. 1995. Interaction of alpha-actinin with the cadherin/catenin cell-cell adhesion complex via alpha-catenin. *J. Cell Biol.* 130:67–77. http://dx.doi.org/10.1083/jcb.130.1.67

Kobielak, A., H.A. Pasolli, and E. Fuchs. 2004. Mammalian formin-1 participates in adherens junctions and polymerization of linear actin cables. *Nat. Cell Biol.* 6:21–30. http://dx.doi.org/10.1038/ncb1075

Kovacs, E.M., M. Goodwin, R.G. Ali, A.D. Paterson, and A.S. Yap. 2002. Cadherin-directed actin assembly: E-cadherin physically associates with the Arp2/3 complex to direct actin assembly in nascent adhesive contacts. *Curr. Biol.* 12:379–382. http://dx.doi.org/10.1016/S0960-9822(02)00661-9

Kovacs, E.M., S. Verma, R.G. Ali, A. Ratheesh, N.A. Hamilton, A. Akhmanova, and A.S. Yap. 2011. N-WASP regulates the epithelial junctional actin cytoskeleton through a non-canonical post-nucleation pathway. *Nat. Cell Biol.* 13:934–943. http://dx.doi.org/10.1038/ncb2290

Kwiatkowski, A.V., S.L. Maiden, S. Pokutta, H.J. Choi, J.M. Benjamin, A.M. Lynch, W.J. Nelson, W.I. Weis, and J. Hardin. 2010. In vitro and in vivo reconstitution of the cadherin-catenin-actin complex from *Caenorhabditis elegans*. *Proc. Natl. Acad. Sci. USA*. 107:14591–14596. http://dx.doi.org/10.1073/pnas.1007349107

Lavin, P.J., R. Gbadegesin, T.V. Damodaran, and M.P. Winn. 2008. Therapeutic targets in focal and segmental glomerulosclerosis. *Curr. Opin. Nephrol. Hypertens.* 17:386–392. http://dx.doi.org/10.1097/MNH.0b013e32830464f4

Lecuit, T., and P.F. Lenne. 2007. Cell surface mechanics and the control of cell shape, tissue patterns and morphogenesis. *Nat. Rev. Mol. Cell Biol.* 8:633–644. http://dx.doi.org/10.1038/nrm2222

Machesky, L.M., and K.L. Gould. 1999. The Arp2/3 complex: A multifunctional actin organizer. *Curr. Opin. Cell Biol.* 11:117–121. http://dx.doi.org/10.1016/S0955-0674(99)80014-3

Mandai, K., H. Nakanishi, A. Satoh, H. Obaishi, M. Wada, H. Nishioka, M. Itoh, A. Mizoguchi, T. Aoki, T. Fujimoto, et al. 1997. Afadin: A novel actin filament–binding protein with one PDZ domain localized at cadherin-based cell-to-cell adherens junction. *J. Cell Biol.* 139:517–528. http://dx.doi.org/10.1083/jcb.139.2.517

Maun, N.A., D.W. Speicher, M.J. DiNubile, and F.S. Southwick. 1996. Purification and properties of a Ca(2+)-independent barbed-end actin filament capping protein, CapZ, from human polymorphonuclear leukocytes. *Biochemistry*. 35:3518–3524. http://dx.doi.org/10.1021/bi952470p

McNeill, H., T.A. Ryan, S.J. Smith, and W.J. Nelson. 1993. Spatial and temporal dissection of immediate and early events following cadherin-mediated epithelial cell adhesion. *J. Cell Biol.* 120:1217–1226. http://dx.doi.org/10.1083/jcb.120.5.1217

Mège, R.M., J. Gavard, and M. Lambert. 2006. Regulation of cell-cell junctions by the cytoskeleton. *Curr. Opin. Cell Biol.* 18:541–548. http://dx.doi.org/10.1016/j.ceb.2006.08.004

Michaud, J.L., K.M. Chaisson, R.J. Parks, and C.R. Kennedy. 2006. FSGS-associated alpha-actinin-4 (K256E) impairs cytoskeletal dynamics in podocytes. *Kidney Int.* 70:1054–1061. http://dx.doi.org/10.1038/sj.ki.5001665

Montell, D.J. 2008. Morphogenetic cell movements: Diversity from modular mechanical properties. *Science*. 322:1502–1505. http://dx.doi.org/10.1126/science.1164073

Morton, W.M., K.R. Ayscough, and P.J. McLaughlin. 2000. Latrunculin alters the actin-monomer subunit interface to prevent polymerization. *Nat. Cell Biol.* 2:376–378. http://dx.doi.org/10.1038/35014075

Nandadasa, S., Q. Tao, N.R. Menon, J. Heasman, and C. Wylie. 2009. N- and E-cadherins in *Xenopus* are specifically required in the neural and non-neural ectoderm, respectively, for F-actin assembly and morphogenetic movements. *Development*. 136:1327–1338. http://dx.doi.org/10.1242/dev.031203

Nolen, B.J., N. Tomasevic, A. Russell, D.W. Pierce, Z. Jia, C.D. McCormick, J. Hartman, R. Sakowicz, and T.D. Pollard. 2009. Characterization of two classes of small molecule inhibitors of Arp2/3 complex. *Nature*. 460:1031–1034. http://dx.doi.org/10.1038/nature08231

Otey, C.A., and O. Carpen. 2004. Alpha-actinin revisited: A fresh look at an old player. *Cell Motil. Cytoskeleton*. 58:104–111. http://dx.doi.org/10.1002/cm.20007

Pasic, L., T. Kotova, and D.A. Schafer. 2008. Ena/VASP proteins capture actin filament barbed ends. *J. Biol. Chem.* 283:9814–9819. http://dx.doi.org/10.1074/jbc.M710475200

Pring, M., A. Weber, and M.R. Bubb. 1992. Profilin-actin complexes directly elongate actin filaments at the barbed end. *Biochemistry*. 31:1827–1836. http://dx.doi.org/10.1021/bi00121a035

Rauzi, M., P. Verant, T. Lecuit, and P.F. Lenne. 2008. Nature and anisotropy of cortical forces orienting *Drosophila* tissue morphogenesis. *Nat. Cell Biol.* 10:1401–1410. http://dx.doi.org/10.1038/ncb1798

Rimm, D.L., E.R. Koslov, P. Kebriaei, C.D. Cianci, and J.S. Morrow. 1995. Alpha 1(E)-catenin is an actin-binding and -bundling protein mediating the attachment of F-actin to the membrane adhesion complex. *Proc. Natl. Acad. Sci. USA*. 92:8813–8817. http://dx.doi.org/10.1073/pnas.92.19.8813

Rizvi, S.A., E.M. Neidt, J. Cui, Z. Feiger, C.T. Skau, M.L. Gardel, S.A. Kozmin, and D.R. Kovar. 2009. Identification and characterization of a small molecule inhibitor of formin-mediated actin assembly. *Chem. Biol.* 16:1158–1168. http://dx.doi.org/10.1016/j.chembiol.2009.10.006

Sawyer, J.K., N.J. Harris, K.C. Slep, U. Gaul, and M. Peifer. 2009. The *Drosophila* afadin homologue Canoe regulates linkage of the actin cytoskeleton to adherens junctions during apical constriction. *J. Cell Biol.* 186:57–73. http://dx.doi.org/10.1083/jcb.200904001

Shankland, S.J. 2006. The podocyte's response to injury: Role in proteinuria and glomerulosclerosis. *Kidney Int.* 69:2131–2147. http://dx.doi.org/10.1038/sj.ki.5000410

Simske, J.S., M. Köppen, P. Sims, J. Hodgkin, A. Yonkof, and J. Hardin. 2003. The cell junction protein VAB-9 regulates adhesion and epidermal morphology in *C. elegans*. *Nat. Cell Biol.* 5:619–625. http://dx.doi.org/10.1038/ncb1002

Solnica-Krezel, L. 2006. Gastrulation in zebrafish — all just about adhesion? *Curr. Opin. Genet. Dev.* 16:433–441. http://dx.doi.org/10.1016/j.gde.2006.06.009

Tang, V.W. 2006. Proteomic and bioinformatic analysis of epithelial tight junction reveals an unexpected cluster of synaptic molecules. *Biol. Direct*. 1:37. http://dx.doi.org/10.1186/1745-6150-1-37

Tao, Q., S. Nandadasa, P.D. McCrea, J. Heasman, and C. Wylie. 2007. G-protein-coupled signals control cortical actin assembly by controlling cadherin expression in the early *Xenopus* embryo. *Development*. 134:2651–2661. http://dx.doi.org/10.1242/dev.002824

Tinkle, C.L., H.A. Pasolli, N. Stokes, and E. Fuchs. 2008. New insights into cadherin function in epidermal sheet formation and maintenance of tissue integrity. *Proc. Natl. Acad. Sci. USA*. 105:15405–15410. http://dx.doi.org/10.1073/pnas.0807374105

Tranter, M.P., S.P. Sugrue, and M.A. Schwartz. 1991. Binding of actin to liver cell membranes: The state of membrane-bound actin. *J. Cell Biol.* 112:891–901. http://dx.doi.org/10.1083/jcb.112.5.891

Turnacioglu, K.K., J.W. Sanger, and J.M. Sanger. 1998. Sites of monomeric actin incorporation in living PtK2 and REF-52 cells. *Cell Motil. Cytoskeleton*. 40:59–70. http://dx.doi.org/10.1002/(SICI)1097-0169(1998)40:1<59::AID-CM6>3.0.CO;2-A

Ulrich, F., and C.P. Heisenberg. 2009. Trafficking and cell migration. *Traffic*. 10:811–818. http://dx.doi.org/10.1111/j.1600-0854.2009.00929.x

Vasioukhin, V., C. Bauer, M. Yin, and E. Fuchs. 2000. Directed actin polymerization is the driving force for epithelial cell-cell adhesion. *Cell*. 100:209–219. http://dx.doi.org/10.1016/S0092-8674(00)81559-7

Weaver, A.M., J.E. Heuser, A.V. Karginov, W.L. Lee, J.T. Parsons, and J.A. Cooper. 2002. Interaction of cortactin and N-WASp with Arp2/3 complex. *Curr. Biol.* 12:1270–1278. http://dx.doi.org/10.1016/S0960-9822(02)01035-7

Weins, A., J.S. Schlondorff, F. Nakamura, B.M. Denker, J.H. Hartwig, T.P. Stossel, and M.R. Pollak. 2007. Disease-associated mutant alpha-actinin-4 reveals a mechanism for regulating its F-actin-binding affinity. *Proc. Natl. Acad. Sci. USA*. 104:16080–16085. http://dx.doi.org/10.1073/pnas.0702451104

Wilkins, J.A., and S. Lin. 1982. High-affinity interaction of vinculin with actin filaments in vitro. *Cell*. 28:83–90. http://dx.doi.org/10.1016/0092-8674(82)90377-4

Xiao, C., S.A. Ogle, M.A. Schumacher, N. Schilling, R.A. Tokhunts, M.A. Orr-Asman, M.L. Miller, D.J. Robbins, F. Hollande, and Y. Zavros. 2010. Hedgehog signaling regulates E-cadherin expression for the maintenance of the actin cytoskeleton and tight junctions. *Am. J. Physiol. Gastrointest. Liver Physiol.* 299:G1252–G1265. http://dx.doi.org/10.1152/ajpgi.00512.2009

Yamada, A., K. Irie, A. Fukuhara, T. Ooshio, and Y. Takai. 2004. Requirement of the actin cytoskeleton for the association of nectins with other cell adhesion molecules at adherens and tight junctions in MDCK cells. *Genes Cells*. 9:843–855. http://dx.doi.org/10.1111/j.1365-2443.2004.00768.x

Yamada, S., S. Pokutta, F. Drees, W.I. Weis, and W.J. Nelson. 2005. Deconstructing the cadherin-catenin-actin complex. *Cell*. 123:889–901. http://dx.doi.org/10.1016/j.cell.2005.09.020

Yamashita, A., K. Maeda, and Y. Maéda. 2003. Crystal structure of CapZ: Structural basis for actin filament barbed end capping. *EMBO J.* 22:1529–1538. http://dx.doi.org/10.1093/emboj/cdg167

Yao, J., T.C. Le, C.H. Kos, J.M. Henderson, P.G. Allen, B.M. Denker, and M.R. Pollak. 2004. Alpha-actinin-4-mediated FSGS: An inherited kidney disease caused by an aggregated and rapidly degraded cytoskeletal protein. *PLoS Biol.* 2:e167. http://dx.doi.org/10.1371/journal.pbio.0020167

Yonemura, S., M. Itoh, A. Nagafuchi, and S. Tsukita. 1995. Cell-to-cell adherens junction formation and actin filament organization: Similarities and differences between non-polarized fibroblasts and polarized epithelial cells. *J. Cell Sci.* 108:127–142.

Yonemura, S., Y. Wada, T. Watanabe, A. Nagafuchi, and M. Shibata. 2010. alpha-Catenin as a tension transducer that induces adherens junction development. *Nat. Cell Biol.* 12:533–542. http://dx.doi.org/10.1038/ncb2055

Young, M.E., J.A. Cooper, and P.C. Bridgman. 2004. Yeast actin patches are networks of branched actin filaments. *J. Cell Biol.* 166:629–635. http://dx.doi.org/10.1083/jcb.200404159

Zhang, J., M. Betson, J. Erasmus, K. Zeikos, M. Bailly, L.P. Cramer, and V.M. Braga. 2005. Actin at cell-cell junctions is composed of two dynamic and functional populations. *J. Cell Sci.* 118:5549–5562. http://dx.doi.org/10.1242/jcs.02639